Search for the associated production of the Higgs boson and a vector boson in proton-proton collisions at $\sqrt{s} = 13$ TeV via Higgs boson decays to τ leptons
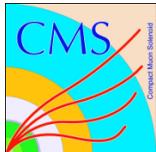
The CMS collaboration

E-mail: cms-publication-committee-chair@cern.ch

ABSTRACT: A search for the standard model Higgs boson produced in association with a W or a Z boson and decaying to a pair of τ leptons is performed. A data sample of proton-proton collisions collected at $\sqrt{s} = 13$ TeV by the CMS experiment at the CERN LHC is used, corresponding to an integrated luminosity of $35.9\,\text{fb}^{-1}$. The signal strength is measured relative to the expectation for the standard model Higgs boson, yielding $\mu = 2.5^{+1.4}_{-1.3}$. These results are combined with earlier CMS measurements targeting Higgs boson decays to a pair of τ leptons, performed with the same data set in the gluon fusion and vector boson fusion production modes. The combined signal strength is $\mu = 1.24^{+0.29}_{-0.27}$ ($1.00^{+0.24}_{-0.23}$ expected), and the observed significance is 5.5 standard deviations (4.8 expected) for a Higgs boson mass of 125 GeV.

https://doi.org/10.1007/JHEP06(2019)093

Contents

1 Introduction

In the standard model (SM), the fermions receive mass via their Yukawa couplings to the Higgs boson [1–9], and measurements of the Higgs boson branching fractions to fermions directly probe these couplings. The Higgs boson decay to a τ lepton pair is particularly interesting because it has the largest branching fraction among the direct leptonic Higgs boson decays ($\mathcal{B}(\mathrm{H} \to \tau^+\tau^-) \simeq 6.3\%$). Many searches for the $\mathrm{H} \to \tau^+\tau^-$ process have been performed by earlier experiments [10–15]. The ATLAS and CMS Collaborations each previously reported evidence for this particular Higgs boson decay process using data collected at center-of-mass energies of 7 and 8 TeV [16–18]. The $\mathrm{H} \to \tau^+\tau^-$ process was measured targeting the gluon fusion and vector boson fusion production modes using data collected by the CMS Collaboration at a center-of-mass energy of 13 TeV [19] resulting in a cross section times branching fraction of $1.09^{+0.27}_{-0.26}$ relative to the SM expectation.

This paper reports on a search for the SM Higgs boson produced in association with a W or a Z boson. The Higgs boson is sought in its decay to a pair of τ leptons. The search is based on a data set of proton-proton (pp) collisions, collected in 2016 by the CMS experiment at a center-of-mass energy of $\sqrt{s} = 13$ TeV, corresponding to an integrated luminosity of $35.9\,\mathrm{fb}^{-1}$. The results are combined with prior results from the CMS $\mathrm{H} \to \tau^+\tau^-$ analysis performed with the same data set and focusing on the gluon fusion and vector boson fusion production modes [19]. This combination provides dedicated signal

regions covering the four leading Higgs boson production mechanisms: gluon fusion, vector boson fusion, W associated production, and Z associated production.

For the ZH associated production channel, $Z \to \ell^+\ell^-$ ($\ell = $ e, μ) decays are considered, combined with four possible $\tau\tau$ final states from the Higgs boson decay: eτ_{h}, $\mu\tau_{\mathrm{h}}$, eμ, and $\tau_{\mathrm{h}}\tau_{\mathrm{h}}$, where τ_{h} denotes τ leptons decaying hadronically. For the WH channel, four final states are considered, with the W boson decaying leptonically to a neutrino and an electron or a muon (listed first in the following notation), and the Higgs boson decaying to at least one τ_{h} (listed second): $\mu+\mu\tau_{\mathrm{h}}$, e$+\mu\tau_{\mathrm{h}}/\mu+e\tau_{\mathrm{h}}$, e$+\tau_{\mathrm{h}}\tau_{\mathrm{h}}$, and $\mu+\tau_{\mathrm{h}}\tau_{\mathrm{h}}$. The final state with an electron, a muon, and a τ_{h} candidate is written as e$+\mu\tau_{\mathrm{h}}/\mu+e\tau_{\mathrm{h}}$ to make clear which light lepton is attributed to the W boson and which to the Higgs boson. The e$+$eτ_{h} final state is not considered because of the lower acceptance and efficiency for electrons with respect to muons. Throughout the paper neutrinos are omitted from the notation of the final states.

2   The CMS detector

The central feature of the CMS apparatus is a superconducting solenoid 6 m in internal diameter, providing a magnetic field of 3.8 T. Within the solenoid volume there are: a silicon pixel and strip tracker, a lead tungstate crystal electromagnetic calorimeter (ECAL), and a brass and scintillator hadron calorimeter (HCAL). Each of these is composed of a barrel and two endcap sections. Forward hadron calorimeters extend the pseudorapidity (η) coverage provided by the barrel and endcap detectors. Muons are detected in gas-ionization chambers embedded in the steel flux-return yoke outside the solenoid. Events are selected using a two-tiered trigger system [20]. A more detailed description of the CMS detector, together with a definition of the coordinate system used and the relevant kinematic variables, can be found in ref. [21].

3   Simulated samples

The signal samples with a Higgs boson produced in association with a W or a Z boson (WH or ZH) are generated at next-to-leading order (NLO) in perturbative quantum chromodynamics (QCD) with the POWHEG 2.0 [22–26] generator extended with the MiNLO procedure [27]. The set of parton distribution functions (PDFs) is NNPDF3.0 [28]. Because the analysis focuses on measuring the WH and ZH processes, the t$\bar{\mathrm{t}}$H process is included as a background. The contribution from Higgs boson events produced via gluon fusion or vector boson fusion is negligible in this analysis. This is because the studied final states, when counting both leptonically and hadronically decaying τ leptons, all include three or four charged lepton candidates. The transverse momentum (p_{T}) distribution of the Higgs boson in the POWHEG simulations is tuned to match closely the next-to-NLO (NNLO) plus next-to-next-to-leading-logarithmic prediction in the HRES 2.3 generator [29, 30]. The production cross sections and branching fractions for the SM Higgs boson production and their corresponding uncertainties are taken from refs. [31–33].

The background samples of t$\bar{\mathrm{t}}$, WZ, and qq $\to$ ZZ are generated at NLO with POWHEG, as are the WH $\to$ WWW, ZH $\to$ ZWW, and H $\to$ ZZ backgrounds. The gg $\to$ ZZ process

is generated at leading order (LO) with MCFM [34]. The MADGRAPH5_AMC@NLO v2.3.3 generator is used for triboson, $t\bar{t}W$, and $t\bar{t}Z$ production, with the jet matching and merging scheme applied either at NLO with the FxFx algorithm [35] or at LO with the MLM algorithm [36]. The generators are interfaced with PYTHIA 8.212 [37] to model the parton showering and fragmentation, as well as the decay of the τ leptons. The PYTHIA parameters affecting the description of the underlying event are set to the CUETP8M1 tune [38].

Generated events are processed through a simulation of the CMS detector based on GEANT4 [39], and are reconstructed with the same algorithms that are used for data. The simulated samples include additional pp interactions per bunch crossing, referred to as pileup. The effect of pileup is taken into account by generating concurrent minimum-bias collision events. The simulated events are weighted such that the distribution of the number of additional pileup interactions matches closely with data. The pileup distribution in data is estimated from the measured instantaneous luminosity for each bunch crossing and results in an average of approximately 23 interactions per bunch crossing.

4   Event reconstruction

The reconstruction of observed and simulated events relies on the particle-flow (PF) algorithm [40]. This algorithm combines information from all subdetectors to identify and reconstruct the particles emerging from pp collisions: charged hadrons, neutral hadrons, photons, muons, and electrons. Combinations of these PF objects are used to reconstruct higher-level objects such as the missing transverse momentum ($\vec{p}_{\mathrm{T}}^{\mathrm{miss}}$). The $\vec{p}_{\mathrm{T}}^{\mathrm{miss}}$ is defined as the projection onto the plane perpendicular to the beam axis of the negative vector sum of the momenta of all reconstructed particle-flow objects in an event. Its magnitude is referred to as $p_{\mathrm{T}}^{\mathrm{miss}}$. The primary pp interaction vertex is taken to be the reconstructed vertex with the largest value of summed p_{T}^2 of jets and the associated $p_{\mathrm{T}}^{\mathrm{miss}}$, calculated from the tracks assigned to the vertex, where the jet finding algorithm is taken from refs. [41, 42] and the associated $\vec{p}_{\mathrm{T}}^{\mathrm{miss}}$ is taken as the negative vector sum of the p_{T} of the jets.

Electrons are identified with a multivariate discriminant combining several quantities describing the track quality, the shape of the energy deposits in the ECAL, and the compatibility of the measurements from the tracker and the ECAL [43]. Muons are reconstructed by combining information from the inner tracker and the muon systems, using two algorithms [44]. One matches tracks in the silicon tracker to hits in the muon detectors, while the other one performs a track fit using hits in both the silicon tracker and the muon systems. To reject nonprompt or misidentified leptons, a relative lepton isolation is defined as:

$$I^{\ell} \equiv \frac{\sum_{\mathrm{charged}} p_{\mathrm{T}} + \max\left(0, \sum_{\mathrm{neutral}} p_{\mathrm{T}} - \frac{1}{2} \sum_{\mathrm{charged,\ PU}} p_{\mathrm{T}}\right)}{p_{\mathrm{T}}^{\ell}}. \tag{4.1}$$

In this expression, $\sum_{\mathrm{charged}} p_{\mathrm{T}}$ is the scalar sum of the transverse momenta of the charged particles originating from the primary vertex and located in a cone of size $\Delta R = \sqrt{(\Delta\eta)^2 + (\Delta\phi)^2} = 0.3\,(0.4)$ centered on the electron (muon) direction, where ϕ is the azimuthal angle in radians. The sum $\sum_{\mathrm{neutral}} p_{\mathrm{T}}$ represents a similar quantity for

neutral particles. The contribution of photons and neutral hadrons originating from pileup vertices is estimated from the scalar sum of the transverse momenta of charged hadrons in the cone originating from pileup vertices, $\sum_{\text{charged, PU}} p_{\text{T}}$. This sum is multiplied by a factor of 1/2, which corresponds approximately to the ratio of neutral to charged hadron production in the hadronization process of inelastic pp collisions, as estimated from simulation. The estimated contribution to I^ℓ from photons and neutral hadrons originating from the primary vertex is required not to be negative, which is enforced by the "max" notation in eq. (4.1). The expression p_{T}^ℓ stands for the p_{T} of the lepton. Isolation requirements used in this analysis include $I^{\text{e}} < 0.10$ and $I^\mu < 0.15$ in the WH channels. In the ZH channels, the isolation criteria are $I^{\text{e}} < 0.15$ ($I^\mu < 0.15$) for electrons (muons) associated to a τ_{h} decay and $I^\mu < 0.25$ for muons associated to a Z boson decay.

Jets are reconstructed with an anti-k_{T} clustering algorithm implemented in the FAST-JET library [42, 45]. It is based on the clustering of neutral and charged PF candidates with a distance parameter of 0.4. Charged PF candidates not associated with the primary vertex of the interaction are not considered when clustering. The combined secondary vertex (CSVv2) algorithm is used to identify jets that are likely to have originated from a bottom quark ("b jets") [46]. The algorithm exploits the track-based lifetime information together with the secondary vertices associated with the jet using a multivariate technique to produce a discriminator for b jet identification. A set of p_{T}-dependent correction factors are applied as weights to simulated events to account for differences in the b tagging efficiency between data and simulation [46]. The working point chosen in this analysis gives an identification efficiency for genuine b jets of about 70% and a misidentification probability for light flavor or gluon jets of about 1%. All events with a b-tagged jet are discarded from this analysis. This selection requirement suppresses the contributions of $t\bar{t}$, $t\bar{t} + W$, and $t\bar{t} + Z$ with minimal impact to the signal selection efficiency.

Hadronically decaying τ leptons are reconstructed with the hadron-plus-strips (HPS) algorithm [47, 48], which is seeded from anti-k_{T} jets. The HPS algorithm reconstructs τ_{h} candidates on the basis of the number of tracks and on the number of ECAL strips with an energy deposit in the η-ϕ plane, in the 1-prong, 1-prong $+ \pi^0$, and 3-prong decay modes. A multivariate analysis (MVA) discriminator [49], including isolation and lifetime information, is used to reduce the rate for quark- and gluon-initiated jets to be identified as τ_{h} candidates. The three working points used in this analysis have efficiencies of about 55, 60, and 65% for genuine τ_{h}, with about 1.0, 1.5, and 2.5% misidentification rates for quark- and gluon-initiated jets, within a p_{T} range typical of a τ_{h} originating from a Z boson. The first working point is used in the $\ell + \tau_{\text{h}}\tau_{\text{h}}$ channels of WH for the τ_{h} that has the same charge as the electron or muon, while the third working point is used for the τ_{h} that has the opposite charge. The second working point is used in the WH channels with exactly one τ_{h}. The third working point is used for all τ_{h} in the ZH channels. Electrons misidentified as τ_{h} candidates are suppressed using a second MVA discriminator that includes tracker and calorimeter information [48]. Muons misidentified as τ_{h} candidates are suppressed using additional cut-based criteria requiring energy and momentum consistency between the measurements in the tracker and the calorimeters, and requiring no more than one segment in the muon detectors [47]. The working points of these discriminators are specific

to each decay channel. The τ_h energy in simulation is corrected for each decay mode on the basis of a measurement of the τ_h energy scale in $Z \to \tau\tau$ events. The rate and the energy of electrons and muons misidentified as τ_h candidates are also corrected in simulation on the basis of a "tag-and-probe" measurement [50] in $Z \to \ell\ell$ events.

In all final states, the visible mass of the Higgs boson candidate, m_{vis}, can be used to separate the $H \to \tau\tau$ signal events from the large irreducible contribution of $Z \to \tau\tau$ events. However, the neutrinos from the τ lepton decays carry a large fraction of the τ lepton energy and reduce the discriminating power of this variable. The SVFIT algorithm [51] combines $\vec{p}_T^{\mathrm{miss}}$ with the four-vector momenta of both τ candidates to estimate the mass of the parent boson, denoted as $m_{\tau\tau}$. The resolution of $m_{\tau\tau}$ is about 20%. The $m_{\tau\tau}$ variable is used for the ZH channels, while m_{vis} is used for the WH channels because the SVFIT algorithm cannot account for the additional $\vec{p}_T^{\mathrm{miss}}$ from the W boson decay.

5 Event selection

Events for the WH and ZH production channels are selected using single- or double-lepton triggers targeting leptonic decays of the W and Z bosons. The trigger and offline selection requirements for all possible decay modes are presented in table 1. Leptons selected by the trigger must be matched to those selected in the analysis. The light leptons (electrons and muons) in the events are required to be separated from each other by $\Delta R > 0.3$, while the τ_h candidates must be separated from each other and from the other leptons by $\Delta R > 0.5$. The resulting event samples are made mutually exclusive by discarding events that have additional identified and isolated electrons or muons.

In the $e + \mu\tau_h / \mu + e\tau_h$ and $\mu + \mu\tau_h$ final states of the WH channel, the two light leptons are required to have the same charge to reduce the $t\bar{t}$ and $Z + $ jets backgrounds where one or more jets is misidentified as a τ_h candidate. The highest p_T light lepton is considered as coming from the W boson. The Higgs boson candidate is formed from the τ_h candidate, which must have opposite charge to the light leptons, and the subleading light lepton. The correct pairing is achieved in about 75% of events, according to simulation. The leading light lepton is required to pass a single-lepton trigger and to have a p_T that is 1 GeV above the online threshold, whereas the subleading light lepton must have $p_T > 15$ GeV, as determined from optimizing for signal sensitivity. In WH associated production, the Higgs and W bosons are dominantly produced back-to-back in ϕ, and may have a longitudinal Lorentz boost that makes them close in η. There is an increased background of misidentified jets at high η because of the decreased detector performance in the endcaps. Considering these characteristics, selection criteria based on three variables have been found to improve the signal sensitivity in both the $e + \mu\tau_h / \mu + e\tau_h$ and $\mu + \mu\tau_h$ final states:

- $L_T > 100$ GeV, where L_T is the scalar sum of p_T of the light leptons and the τ_h candidate;

- $|\Delta\phi(\ell_1, H)| > 2.0$, where ℓ_1 is the leading light lepton, and H is the system formed by the subleading light lepton and the τ_h candidate;

- $|\Delta\eta(\ell_1, H)| < 2.0$.

WH selection
τ_h baseline requirements: $p_\mathrm{T}^{\tau_\mathrm{h}} > 20\,\mathrm{GeV}$, $|\eta^{\tau_\mathrm{h}}| < 2.3$
e baseline requirements: $p_\mathrm{T}^\mathrm{e} > 15\,\mathrm{GeV}$, $|\eta^\mathrm{e}| < 2.5$, e ID 80% efficiency, $I^\mathrm{e} < 0.10$
μ baseline requirements: $p_\mathrm{T}^\mu > 15\,\mathrm{GeV}$, $|\eta^\mu| < 2.4$, μ ID $> 99\%$ efficiency, $I^\mu < 0.15$

Channel	Trigger ($p_\mathrm{T}(\mathrm{GeV})/|\eta|$)	Light lepton selection	τ_h selection
$\mathrm{e}+\mu\tau_\mathrm{h}/\mu+\mathrm{e}\tau_\mathrm{h}$	$\mathrm{e}(25/2.1)$ or $\mu(22/2.1)$	$p_\mathrm{T}^\mathrm{e} > 26\,\mathrm{GeV}$ or $p_\mathrm{T}^\mu > 23\,\mathrm{GeV}$	τ_h isolation 60% eff.
$\mu+\mu\tau_\mathrm{h}$	$\mu(22/2.1)$	$p_\mathrm{T}^\mu > 23\,\mathrm{GeV}$	τ_h isolation 60% eff.
$\mathrm{e}+\tau_\mathrm{h}\tau_\mathrm{h}$	$\mathrm{e}(25/2.1)$	$p_\mathrm{T}^\mathrm{e} > 26\,\mathrm{GeV}$	τ_h isolation 55 or 65% eff.
$\mu+\tau_\mathrm{h}\tau_\mathrm{h}$	$\mu(22/2.1)$	$p_\mathrm{T}^\mu > 23\,\mathrm{GeV}$	τ_h isolation 55 or 65% eff.

ZH selection
Z boson reconstructed from opposite charge, same-flavor light leptons, $60 < m_{\ell\ell} < 120\,\mathrm{GeV}$
τ_h baseline requirements: $p_\mathrm{T}^{\tau_\mathrm{h}} > 20\,\mathrm{GeV}$, $|\eta^{\tau_\mathrm{h}}| < 2.3$, τ_h isolation 65% efficiency
e baseline requirements: $p_\mathrm{T}^\mathrm{e} > 10\,\mathrm{GeV}$, $|\eta^\mathrm{e}| < 2.5$, e ID 90% efficiency
μ baseline requirements: $p_\mathrm{T}^\mu > 10\,\mathrm{GeV}$, $|\eta^\mu| < 2.4$, μ ID $> 99\%$ efficiency, $I^\mu < 0.25$

Channel	Trigger ($p_\mathrm{T}(\mathrm{GeV})/|\eta|$)	$\mathrm{Z} \to \ell\ell$ lepton selection	$\mathrm{H} \to \tau\tau$ lepton selection
$\mathrm{ee}+\mu\tau_\mathrm{h}$			$I^\mu < 0.15$
$\mathrm{ee}+\mathrm{e}\tau_\mathrm{h}$	$[\mathrm{e}_1(23/2.5)\,\&\,\mathrm{e}_2(12/2.5)]$	$[p_\mathrm{T}^{\mathrm{e}_1} > 24\,\mathrm{GeV}\,\&\,p_\mathrm{T}^{\mathrm{e}_2} > 13\,\mathrm{GeV}]$	e ID 80% eff., $I^\mathrm{e} < 0.15$
$\mathrm{ee}+\tau_\mathrm{h}\tau_\mathrm{h}$	or $\mathrm{e}_1(27/2.5)$	or $p_\mathrm{T}^{\mathrm{e}_1} > 28\,\mathrm{GeV}$	baseline selection listed above
$\mathrm{ee}+\mathrm{e}\mu$			e ID 80% eff., $I^\mathrm{e} < 0.15$, $I^\mu < 0.15$
$\mu\mu+\mu\tau_\mathrm{h}$			$I^\mu < 0.15$
$\mu\mu+\mathrm{e}\tau_\mathrm{h}$	$[\mu_1(17/2.4)\,\&\,\mu_2(8/2.4)]$	$[p_\mathrm{T}^{\mu_1} > 18\,\mathrm{GeV}\,\&\,p_\mathrm{T}^{\mu_2} > 10\,\mathrm{GeV}]$	e ID 80% eff., $I^\mathrm{e} < 0.15$
$\mu\mu+\tau_\mathrm{h}\tau_\mathrm{h}$	or $\mu_1(24/2.4)$	or $p_\mathrm{T}^{\mu_1} > 25\,\mathrm{GeV}$	baseline selection listed above
$\mu\mu+\mathrm{e}\mu$			e ID 80% eff., $I^\mathrm{e} < 0.15$, $I^\mu < 0.15$

Table 1. Kinematic selection requirements for WH and ZH events. The trigger requirement is defined by a combination of trigger candidates with p_T over a given threshold (in GeV), indicated inside parentheses. The $|\eta|$ thresholds come from trigger and object reconstruction constraints. ZH events are selected with either a lower p_T threshold double lepton trigger or a higher p_T threshold single lepton trigger.

In the $\mathrm{e} + \tau_\mathrm{h}\tau_\mathrm{h}$ and $\mu + \tau_\mathrm{h}\tau_\mathrm{h}$ final states of the WH channel, the τ_h candidates are required to have opposite charge. The τ_h candidate that has the same charge as the light lepton must have $p_\mathrm{T} > 35\,\mathrm{GeV}$, while the other one is required to have $p_\mathrm{T} > 20\,\mathrm{GeV}$. This requirement is driven by the fact that the τ_h candidate with the same charge as the light lepton is often a jet misidentified as a τ_h from the SM background, and the jet misidentification rate strongly decreases as p_T increases. Selection criteria based on three variables have been found to improve the results in the $\mathrm{e} + \tau_\mathrm{h}\tau_\mathrm{h}$ and $\mu + \tau_\mathrm{h}\tau_\mathrm{h}$ final states:

- $L_\mathrm{T} > 130\,\mathrm{GeV}$, where L_T is the scalar sum of p_T of the light lepton and τ_h candidates;

- $|\vec{S_\mathrm{T}}| < 70\,\mathrm{GeV}$, where $\vec{S_\mathrm{T}}$ is the vector sum of p_T of the light lepton, τ_h candidates, and $\vec{p}_\mathrm{T}^{\,\mathrm{miss}}$;

- $|\Delta\eta(\tau_\mathrm{h}, \tau_\mathrm{h})| < 2.0$.

In the ZH final states, the Z boson is reconstructed from the opposite charge, same-flavor light lepton combination that has a mass closest to the Z boson mass. Different identification and isolation selections are applied to the light leptons associated to the Z boson compared with those associated to the Higgs boson. The selections are looser for those associated with the Z boson to increase the signal acceptance, while tighter selections are applied to the light leptons assigned to the Higgs boson to decrease the background contributions from Z+jets and other reducible backgrounds. The leptons assigned to the Higgs boson are required to have opposite charge. The specific selections detailed in table 1, including those chosen for the τ_h candidates, were optimized to obtain the best expected signal sensitivity.

Candidates for associated ZH production are also categorized depending on the value of L_T^{Higgs}, defined as the scalar sum of p_T of the visible decay products of the Higgs boson. The large Higgs boson mass causes the decay products to have relatively high p_T compared to the jets misidentified as leptons from the $Z + \text{jets}$ background process, which leads to a higher signal purity in the category with high L_T^{Higgs}. The thresholds to separate the high L_T^{Higgs} and low L_T^{Higgs} regions are optimized to maximize the expected signal sensitivity for each $H \to \tau\tau$ final state. The threshold is equal to $50\,\text{GeV}$ in the $\ell\ell + e\mu$ final states, $60\,\text{GeV}$ in the $\ell\ell + e\tau_h$ and $\ell\ell + \mu\tau_h$ final states, and $75\,\text{GeV}$ in the $\ell\ell + \tau_h\tau_h$ final state.

6   Background estimation

The irreducible backgrounds (ZZ, t$\bar{\text{t}}$Z, WWZ, WZZ, ZZZ, as well as WZ and t$\bar{\text{t}}$W in the WH channels) are estimated from simulation and scaled by their theoretical cross sections at the highest order available. Inclusive Higgs boson decays to W or Z boson pairs and the t$\bar{\text{t}}$H associated production background processes are also estimated from simulation.

The reducible backgrounds, which have at least one jet misidentified as an electron, muon, or τ_h candidate, are estimated from data. The dominant reducible background contributions come from t$\bar{\text{t}}$ and $Z + \text{jets}$ in the WH channels and from t$\bar{\text{t}}$, $Z + \text{jets}$, and $WZ + \text{jets}$ in the ZH channels. Misidentification rates are estimated in control samples that specifically measure the rate at which jets pass the identification criteria used for each τ candidate (electrons, muons, or τ_h). The misidentification rates are then applied to reweight events with τ candidates failing the identification criteria but passing all other signal region selections. These reweighted events estimate the contribution from processes with jets misidentified as τ candidates in the signal region.

In the WH analysis, the misidentification rate of jets as τ candidates is measured in Z+jets events. After reconstructing the $Z \to \text{ee}$ decay, the jet-to-muon misidentification rate is estimated as a function of the lepton p_T by applying the lepton identification algorithm to any additional jet in the event. Similarly, $(Z \to \mu\mu) + \text{jets}$ events are used to estimate the jet-to-electron and jet-to-τ_h misidentification rates. Events where the τ candidates arise from genuine leptons, primarily from the WZ process, are estimated from simulation and subtracted from the data so that the misidentification rates are measured for jets only. The rates are measured in bins of lepton p_T, and are separated by the reconstructed decay mode of the τ_h candidates.

In the e+$\mu\tau_\text{h}$/μ+eτ_h and μ+$\mu\tau_\text{h}$ final states, events that do not pass the identification conditions of either the subleading light lepton or the τ_h are reweighted to estimate the reducible background contribution in the signal region. In particular, events with exactly one object failing the identification criteria receive a weight $f/(1-f)$, where f is the misidentification rate for the particular type of object. Events with both objects failing the identification criteria receive a weight $-f_1 f_2/[(1-f_1)(1-f_2)]$, where the negative sign removes the double counting of events with two jets. This method estimates the number of events for which the subleading light lepton or the τ_h candidate corresponds to a jet. Such events are therefore removed from simulated samples to avoid double counting. However, events that have a jet misidentified as the leading lepton, but two genuine leptons for the subleading lepton and the τ_h, are not taken into account with the misidentification rate method and are therefore estimated from simulation. These events mostly arise from $t\bar{t}$ and Z+jets processes, and account for less than 10% of the total expected background in the signal region. In the e + $\tau_\text{h}\tau_\text{h}$ and μ + $\tau_\text{h}\tau_\text{h}$ final states of the WH channels, the method is essentially the same, except that the misidentification rate functions are applied only to events where the τ_h candidate that has the same charge as the light lepton fails the identification criteria.

In the ZH analysis, a very similar method is used to estimate the contribution of jets misidentified as electrons, muons, or τ_h candidates in the signal region. The misidentification rates are measured in a region with an opposite-charge same-flavor lepton pair compatible with a Z boson, and two additional objects. This region is dominated by Z + jets events with a small contribution from $t\bar{t}$ events. In a procedure identical to that of the WH final states, the contribution from genuine leptons is estimated from simulation and is subtracted, and the rates are measured in bins of lepton p_T and are split between reconstructed decay modes for the τ_h candidates. In the ZH analysis, events that pass the full signal region selection with the exception that either or both of the τ candidates associated to the Higgs boson fail the identification criteria are weighted as a function of the misidentification rates. To avoid double counting, events with both τ candidates failing the selection criteria have their weight subtracted from the events that have only a single object failing. This misidentification rate method is used to estimate only the yield of the reducible backgrounds. The $m_{\tau\tau}$ distribution of the reducible background contribution is taken from data in a region with negligible signal and irreducible background contribution, defined similarly to the signal region but with same charge τ candidates passing relaxed identification and isolation criteria.

7   Systematic uncertainties

The overall uncertainty in the τ_h identification efficiency for genuine τ_h leptons is 5% [48], which has been measured with a tag-and-probe method in Z $\to \tau\tau$ events. An uncertainty of 1.2% in the visible energy of genuine τ_h leptons affects both the shape and yield of the final mass distributions for the signals and backgrounds. It is uncorrelated among the 1-prong, 1-prong + π^0, and 3-prong decay modes.

The uncertainties in the electron and muon identification, isolation, and trigger efficiencies lead to a rate uncertainty of 2% for both electrons and muons. The uncertainty in

the electron energy, which amounts to 2.5% in the endcaps and 1% in the barrel, affects both the shape and yield of the final mass distributions. In all channels, the effect of the uncertainty in the muon energy is negligible.

The rate uncertainty related to discarding events with a b-tagged jet is 4.5% for processes with heavy-flavor jets, and 0.15% for processes with light-flavor jets.

Theoretical uncertainties associated with finite-order perturbative calculations, and with the choice of the PDF set, are taken into account for the ZZ and WZ background processes. The theoretical uncertainties are evaluated by varying renormalization and factorization scales by factors of 0.5 and 2.0, independently. The process leads to yield uncertainties of $^{+3.2\%}_{-4.2\%}$ for the qq $\to$ ZZ process, and $\pm 3.2\%$ for the WZ process. The uncertainty from the PDF set is determined to be $^{+3.1\%}_{-4.2\%}$ for the qq $\to$ ZZ process, and $\pm 4.5\%$ for the WZ process. In addition, a 10% uncertainty in the NLO K factor used for the gg $\to$ ZZ prediction is used [52]. The uncertainties in the cross section of the rare $t\bar{t}W$ and $t\bar{t}Z$ processes amount to 25% [53].

The rate and acceptance uncertainties for the signal processes related to the theoretical calculations arise from uncertainties in the PDFs, variations of the QCD renormalization and factorization scales, and uncertainties in the modeling of parton showers. The magnitude of the rate uncertainty is estimated from simulation and depends on the production process. The inclusive uncertainties related to the PDFs amount to 1.9 and 1.6%, respectively, for the WH and ZH production modes [31]. The corresponding uncertainty for the variation of the renormalization and factorization scales is 0.7 and 3.8%, respectively [31].

The reducible backgrounds are estimated by using the measured rates for jets to be misidentified as electron, muon, or $\tau_{\rm h}$ candidates. In the WH channels, an uncertainty arises from potentially different misidentification rates in Z + jets events, where the rates are measured, and in W + jets or $t\bar{t}$ events, which constitute a large fraction of the reducible background in the signal region. This leads to a 20% yield uncertainty for the reducible background in each final state of the WH analysis. This uncertainty also covers the measured differences in observed versus predicted reducible background yields in multiple dedicated control regions.

In the ZH final states a similar uncertainty is applied based on potential differences between the region where the misidentification rates are measured and the region where they are applied. These uncertainties are based on the results of closure tests comparing the differences in observed versus predicted reducible background yields. The uncertainty is taken to be the largest difference between simulation-based and data-based closure tests. The yield uncertainties are 50% in the $\ell\ell + e\tau_{\rm h}$ final states, 25% in $\ell\ell + \mu\tau_{\rm h}$, 40% in $\ell\ell + \tau_{\rm h}\tau_{\rm h}$, and 100% in $\ell\ell + e\mu$. The large uncertainty in the $\ell\ell + e\mu$ final states results from the very low expected reducible background yields, which makes the closure tests susceptible to large statistical fluctuations.

The misidentification rates of jets as τ candidates are measured in different bins of lepton $p_{\rm T}$, separately for the three reconstructed decay modes for the $\tau_{\rm h}$ candidate. In the WH channels, where the mass distribution for the reducible background is taken from the misidentification rate method, the statistical uncertainty in every bin is considered as an

independent uncertainty and is propagated to the mass distributions and to the yields of the reducible background estimate. In contrast, in the ZH channels, the mass distribution of the reducible background is estimated from data in a region where the τ candidates have the same charge and pass relaxed isolation conditions. Therefore, the statistical uncertainties in the misidentification rates do not have an impact on the shape of the mass distribution in this channel. Additionally, their impact on the reducible background yields is subleading compared to the closure-based uncertainties. In both the WH and ZH channels, an additional uncertainty in the misidentification rates arising from the subtraction of prompt leptons estimated from simulation is taken into account and propagated to the reducible background mass distributions.

The $\vec{p}_{\mathrm{T}}^{\mathrm{miss}}$ scale uncertainties [54], which are computed event-by-event, affect the normalization of various processes through the event selection, as well as their distributions through the propagation of these uncertainties to the di-τ mass $m_{\tau\tau}$ in the ZH channels. The $\vec{p}_{\mathrm{T}}^{\mathrm{miss}}$ scale uncertainties arising from unclustered energy deposits in the detector come from four independent sources related to the tracker, ECAL, HCAL, and forward calorimeters. Additionally, $\vec{p}_{\mathrm{T}}^{\mathrm{miss}}$ scale uncertainties related to the uncertainties in the jet energy measurement, which affect the $\vec{p}_{\mathrm{T}}^{\mathrm{miss}}$ calculation, are taken into account.

Uncertainties related to the finite number of simulated events, or to the limited number of events in data control regions, are taken into account. They are considered for all bins of the distributions used to extract the results. They are uncorrelated across different samples, and across bins of a single distribution. Finally, the uncertainty in the integrated luminosity amounts to 2.5% [55]. The systematic uncertainties considered in the analysis are summarized in table 2.

8   Results

The results of the analysis are extracted with a global maximum likelihood fit based on the reconstructed Higgs boson mass distributions in the eight ZH and four WH signal regions. In the ZH channels, the $m_{\tau\tau}$ distribution is used. The $m_{\tau\tau}$ distributions are shown in figure 1 for each of the four H $\to \tau\tau$ final states, and in figure 2 for all eight ZH channels combined together. The low $L_{\mathrm{T}}^{\mathrm{Higgs}}$ and high $L_{\mathrm{T}}^{\mathrm{Higgs}}$ regions are plotted side-by-side. The eight ZH channels are each fit as separate distributions in the global fit; combining them together is for visualization purposes only. The WH and ZH signal yields correspond to their best fit signal strength value of 2.5. The distributions are shown after the fit and include both statistical and systematic uncertainties. The signal and background predicted yields, as well as the number of observed events, are given for each of the four H $\to \tau\tau$ final states of the ZH channel in table 3.

The results in the WH channels are obtained from the distributions of the visible mass of the τ_{h} candidate pairs in the $\ell + \tau_{\mathrm{h}}\tau_{\mathrm{h}}$ channels, and of the visible mass of the τ_{h} and subleading light lepton in the $\ell + \ell\tau_{\mathrm{h}}$ final states. The mass distributions are shown in figure 3 for the semileptonic and hadronic channels. Figure 4 shows all four WH channels combined together. The signal and background predicted yields, as well as the number of observed events, are given for each final state for the WH channel in table 4.

Source of uncertainty	Magnitude	Process
τ_{h} ID & isolation	5%	All simulations
τ_{h} energy† (1.2% energy shift)	0.1–1.9%	All simulations
e ID & isolation & trigger	2%	All simulations
e energy† (1–2.5% energy shift)	0.3–1.4%	All simulations
μ ID & isolation & trigger	2%	All simulations
b veto	0.15–4.50%	All simulations
Diboson theoretical uncertainty	5%	WZ, ZZ
$gg \to ZZ$ NLO K factor	10%	$gg \to ZZ$
$t\bar{t}+W/Z$ theoretical uncertainty	25%	$t\bar{t}+W/Z$
Signal theoretical uncertainty	Up to 4%, see text	Signal
Reducible background uncertainties:		Reducible bkg.
WH statistical error propagation†	1–2%	
WH prompt lepton normalization†	2.6% in e+$\mu\tau_{\mathrm{h}}/\mu$+eτ_{h}, 4% in μ+$\mu\tau_{\mathrm{h}}$	
ZH prompt lepton normalization†	20% in $\ell\ell$+eμ, <1% elsewhere	
WH normalization	20%	
ZH normalization	25–100%	
$\vec{p}_{\mathrm{T}}^{\mathrm{miss}}$ energy†	Up to 1.5% in WH, <1% in ZH	All simulations
Limited number of events	Stat. uncertainty per bin	All
Integrated luminosity	2.5%	All simulations

Table 2. Sources of systematic uncertainty. The sign † marks the uncertainties that are both shape- and rate-based. Uncertainties that affect only the normalizations have no marker. For the shape and normalization uncertainties, the magnitude column lists the range of the associated change in normalization, which varies by process and final state. The last column specifies the processes affected by each source of uncertainty.

Events from all final states are combined as a function of their decimal logarithm of the ratio of the signal (S) to signal-plus-background ($S + B$) in each bin, as shown in figure 5. Most of the ZH and WH final states contribute to the most sensitive bins in this distribution. The sensitive bins in the mass distributions correspond to those that include the peak of the signal from approximately 70–110 GeV in the m_{vis} distributions from the WH channels and 100–160 GeV in the $m_{\tau\tau}$ distributions from the ZH channels. The least sensitive bins in figure 5 include background events from all channels away from the signal peak and especially in the low $L_{\mathrm{T}}^{\mathrm{Higgs}}$ region for the ZH channels. An excess of observed events with respect to the SM background expectation is visible in the most sensitive bins of the analysis.

The maximum likelihood fit to the WH and ZH associated production event distributions yields a signal strength $\mu = 2.5^{+1.4}_{-1.3}$ ($1.0^{+1.1}_{-1.0}$ expected) for a significance of 2.3 standard deviations (1.0 expected). The large μ value is driven by the WH channels, where the observation significantly exceeds the expectations from the SM including the Higgs boson. The constraints from the combined global fit are used to extract the individual best fit signal strengths for WH and ZH: $\mu_{\mathrm{WH}} = 3.6^{+1.8}_{-1.6}$ ($1.0^{+1.6}_{-1.4}$ expected), and $\mu_{\mathrm{ZH}} = 1.4^{+1.6}_{-1.5}$ ($1.0^{+1.5}_{-1.3}$ expected).

Process	$\ell\ell + e\tau_h$	$\ell\ell + \mu\tau_h$	$\ell\ell + \tau_h\tau_h$	$\ell\ell + e\mu$
ZZ	14.40 ± 0.36	26.91 ± 0.55	25.58 ± 1.05	9.33 ± 0.18
Reducible	14.01 ± 1.55	17.58 ± 1.17	58.05 ± 2.87	3.66 ± 4.60
Other	0.62 ± 0.08	1.54 ± 0.61	0.81 ± 0.42	3.02 ± 0.23
Total backgrounds	29.03 ± 1.59	46.03 ± 1.43	84.44 ± 3.08	16.01 ± 4.61
$WH, H \to \tau\tau$	0.008 ± 0.002	0.010 ± 0.003	0.016 ± 0.005	0.002 ± 0.001
$ZH, H \to \tau\tau$	2.83 ± 0.39	5.31 ± 0.70	5.29 ± 1.17	1.62 ± 0.20
Total signal	2.84 ± 0.39	5.32 ± 0.70	5.31 ± 1.17	1.62 ± 0.20
Observed	33	53	87	20

Table 3. Background and signal expectations for the ZH channels, together with the numbers of observed events, for the post-fit signal region distributions. The ZH final states are each grouped according to the Higgs boson decay products. The $\ell\ell$ notation covers both $Z \to \mu\mu$ and $Z \to ee$ events. The WH and ZH, $H \to \tau\tau$ signal yields are listed both individually and summed together, and correspond to $H \to \tau\tau$ with a best fit $\mu = 2.5$ for a Higgs boson with a mass $m_H = 125\,\text{GeV}$. The background uncertainty accounts for all sources of background uncertainty, systematic as well as statistical, after the global fit. The contribution from "Other" includes events from triboson, $t\bar{t} + W/Z$, $t\bar{t}H$ production, and all production modes leading to $H \to WW$ and $H \to ZZ$ decays.

Process	$e + \mu\tau_h/\mu + e\tau_h$	$\mu + \mu\tau_h$	$e + \tau_h\tau_h$	$\mu + \tau_h\tau_h$
ZZ	1.56 ± 0.05	0.93 ± 0.03	0.82 ± 0.04	1.18 ± 0.05
WZ	7.92 ± 0.28	6.69 ± 0.24	4.83 ± 0.25	8.38 ± 0.42
Reducible	10.09 ± 1.61	12.19 ± 1.72	10.68 ± 1.27	19.80 ± 1.87
Other	2.28 ± 0.61	3.77 ± 0.84	1.71 ± 1.08	1.76 ± 0.90
Total backgrounds	21.85 ± 1.75	23.58 ± 1.93	18.04 ± 1.69	31.12 ± 2.12
$WH, H \to \tau\tau$	4.28 ± 0.72	4.25 ± 0.73	3.51 ± 0.62	5.45 ± 0.97
$ZH, H \to \tau\tau$	0.42 ± 0.07	0.40 ± 0.08	0.33 ± 0.07	0.44 ± 0.10
Total signal	4.70 ± 0.72	4.65 ± 0.73	3.84 ± 0.62	5.89 ± 0.98
Observed	28	29	23	38

Table 4. Background and signal expectations for the WH channels, together with the numbers of observed events, for the post-fit signal region distributions. The WH and ZH, $H \to \tau\tau$ signal yields are listed both individually and summed together, and correspond to $H \to \tau\tau$ with a best fit $\mu = 2.5$ for a Higgs boson with a mass $m_H = 125\,\text{GeV}$. The background uncertainty accounts for all sources of background uncertainty, systematic as well as statistical, after the global fit. The contributions from triboson, $t\bar{t} + W/Z$, $t\bar{t}H$ production, and all production modes leading to $H \to WW$ and $H \to ZZ$ decays are included in the category labeled "Other".
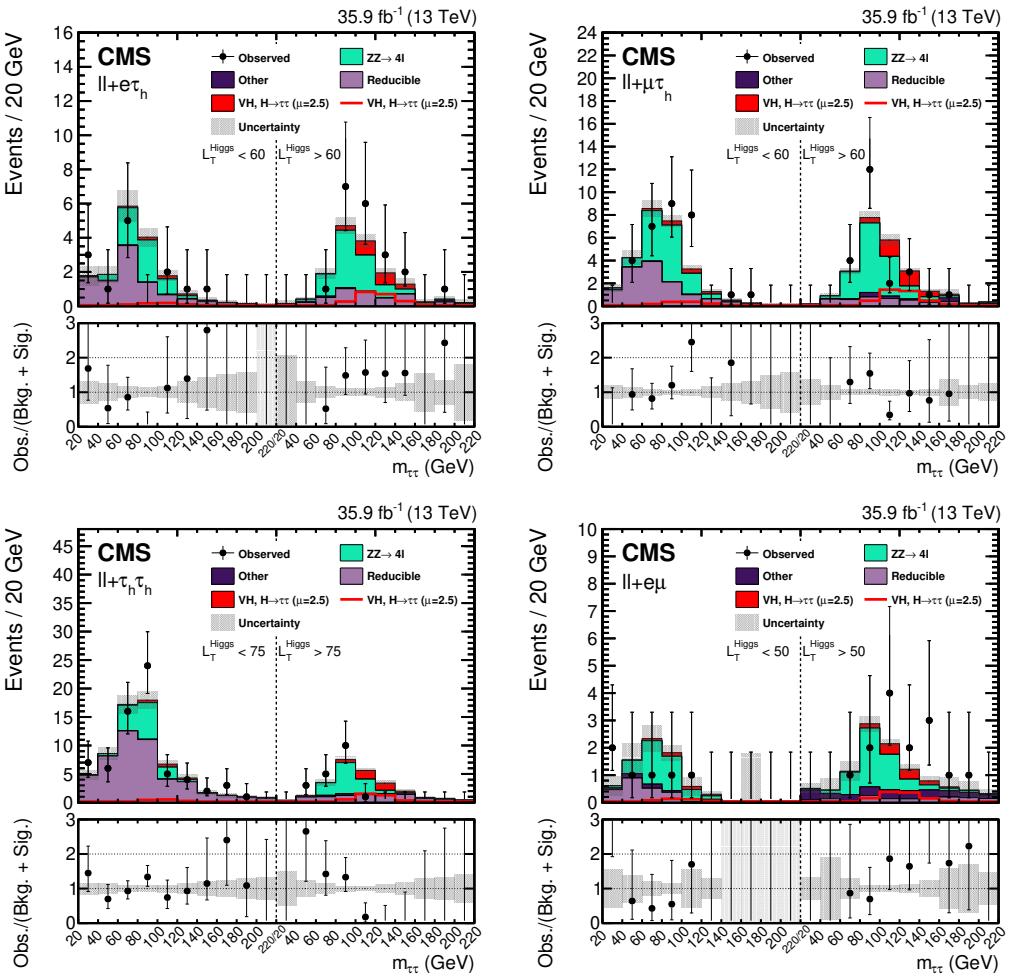
Figure 1. The post-fit $m_{\tau\tau}$ distributions used to extract the signal shown for (upper left) $\ell\ell + \mathrm{e}\tau_\mathrm{h}$, (upper right) $\ell\ell + \mu\tau_\mathrm{h}$, (lower left) $\ell\ell + \tau_\mathrm{h}\tau_\mathrm{h}$, and (lower right) $\ell\ell + \mathrm{e}\mu$. The uncertainties include both statistical and systematic components. The left half of each distribution is the low $L_\mathrm{T}^\mathrm{Higgs}$ region, while the right half of each distribution is the high $L_\mathrm{T}^\mathrm{Higgs}$ region. The WH and ZH, H $\to \tau\tau$ signal processes are summed together and shown as VH, H $\to \tau\tau$ with a best fit $\mu = 2.5$. VH, H $\to \tau\tau$ is shown both as a stacked filled histogram and an open overlaid histogram. The contribution from "Other" includes events from triboson, $\mathrm{t\bar{t}}+\mathrm{W/Z}$, $\mathrm{t\bar{t}H}$ production, and all production modes leading to H $\to$ WW and H $\to$ ZZ decays. In these distributions the ZH, H $\to \tau\tau$ process contributes more than 99% of the total of VH, H $\to \tau\tau$.

The results of this dedicated WH and ZH associated production analysis are combined with the prior H $\to \tau\tau$ analysis that targeted the gluon fusion and vector boson fusion production modes using the same data set and dilepton final states [19]. The signal regions in both analyses are orthogonal by design because events with extra leptons are removed from the gluon fusion and vector boson fusion targeted dilepton final states. Changes in the gluon fusion signal modeling and uncertainties were made between the publication of ref. [19] and the combination presented here, to take advantage of the most accurate, available simulations of the gluon fusion process. The gluon fusion simulation used in
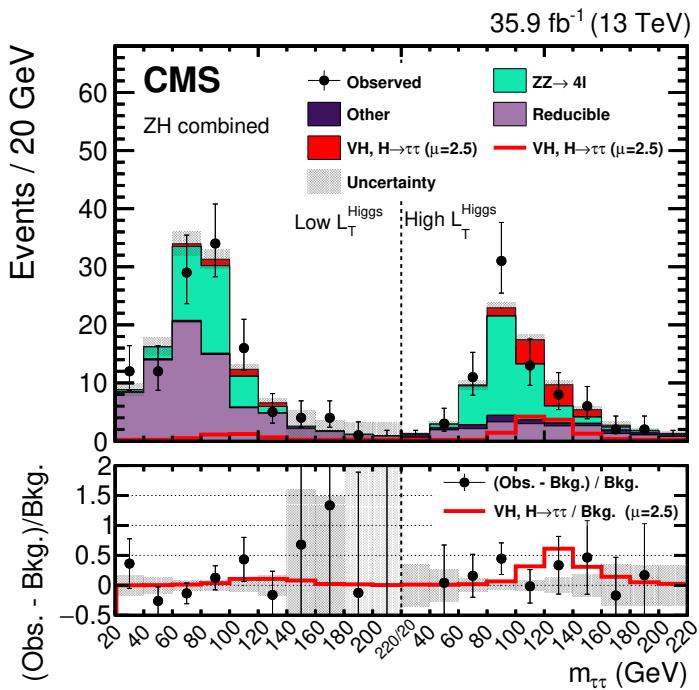
Figure 2. The post-fit $m_{\tau\tau}$ distributions used to extract the signal, shown for all 8 ZH channels combined. The uncertainties include both statistical and systematic components. The left half of the distribution is the low L_T^{Higgs} region, while the right half corresponds to the high L_T^{Higgs} region. The definitions of the L_T^{Higgs} regions in this distribution are the same as those used in figure 1 and are final state dependent. The WH and ZH, $H \to \tau\tau$ signal processes are summed together and shown as VH, $H \to \tau\tau$ with a best fit $\mu = 2.5$. VH, $H \to \tau\tau$ is shown both as a stacked filled histogram and an open overlaid histogram. The contribution from "Other" includes events from triboson, $t\bar{t} + W/Z$, $t\bar{t}H$ production, and all production modes leading to $H \to WW$ and $H \to ZZ$ decays. In this distribution the ZH, $H \to \tau\tau$ process contributes more than 99% of the total of VH, $H \to \tau\tau$.

ref. [19] was computed with next-to-leading order matrix elements merged with the parton shower (NLO + PS) accuracy. These NLO + PS gluon fusion samples were reweighted to match the Higgs boson p_T spectrum from the NNLOPS generator [56]. Additionally, the gluon fusion cross section uncertainty scheme has been updated to the one proposed in ref. [31]. This uncertainty scheme includes 9 nuisance parameters accounting for the uncertainties in the cross section prediction for exclusive jet bins, the 2-jet and 3-jet VBF phase space regions, different Higgs boson p_T regions, and the uncertainty in the Higgs boson p_T distribution due to missing higher-order corrections relating to the treatment of the top quark mass.

After applying the mentioned changes to the gluon fusion modeling, the gluon fusion and VBF targeted analysis results in a best fit signal strength for $H \to \tau\tau$ of $\mu = 1.17^{+0.27}_{-0.25}$ ($1.00^{+0.25}_{-0.23}$ expected).

With combined results, the significance, signal strengths, and Higgs boson couplings can be measured with better precision than with either analysis alone. The combination

JHEP06(2019)093
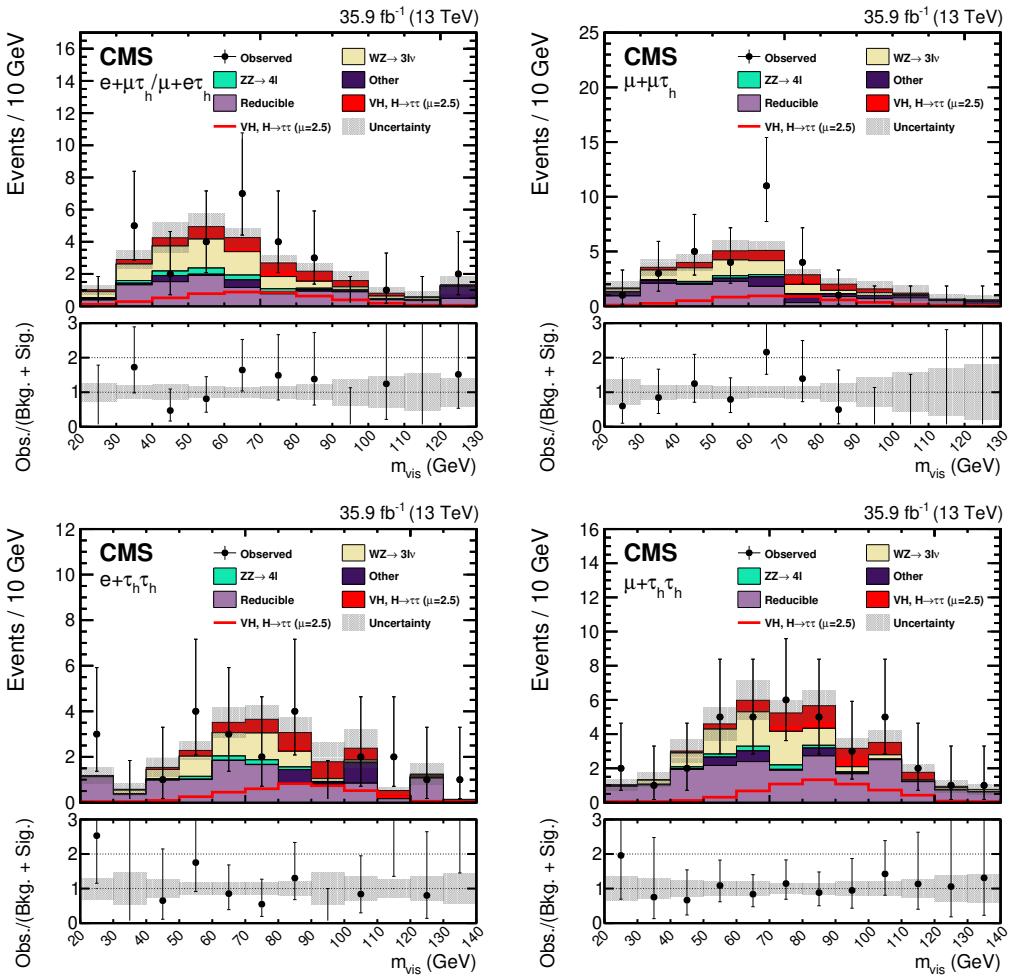
Figure 3. Post-fit visible mass distributions of the Higgs boson candidate in the $e + \mu\tau_h/\mu + e\tau_h$ (upper left), $\mu + \mu\tau_h$ (upper right), $e + \tau_h\tau_h$ (lower left), and $\mu + \tau_h\tau_h$ (lower right) final states. The uncertainties include both statistical and systematic components. The WH and ZH, $H \to \tau\tau$ signal processes are summed together and shown as VH, $H \to \tau\tau$ with a best fit $\mu = 2.5$. VH, $H \to \tau\tau$ is shown both as a stacked filled histogram and an open overlaid histogram. The contribution from "Other" includes events from triboson, $t\bar{t} + W/Z$, $t\bar{t}H$ production, and all production modes leading to $H \to WW$ and $H \to ZZ$ decays. In these distribution the WH, $H \to \tau\tau$ processes contributes 91–93% of the total of VH, $H \to \tau\tau$.

leads to an observed significance of 5.5 standard deviations (4.8 expected). The best fit signal strength for the combination is $\mu = 1.24^{+0.29}_{-0.27}$ ($1.00^{+0.24}_{-0.23}$ expected). The signal regions used in the combination target the four leading Higgs boson production mechanisms allowing extraction of the Higgs boson signal strength per production mechanism. The production mode specific signal strength measurements are shown in figure 6.

This combination places a tighter constraint on the $H \to \tau\tau$ process in the (κ_V, κ_f) Higgs boson couplings parameter space than previous analyses targeting exclusively the $H \to \tau\tau$ decay process. The coupling parameters κ_V and κ_f quantify, respectively, the ratio
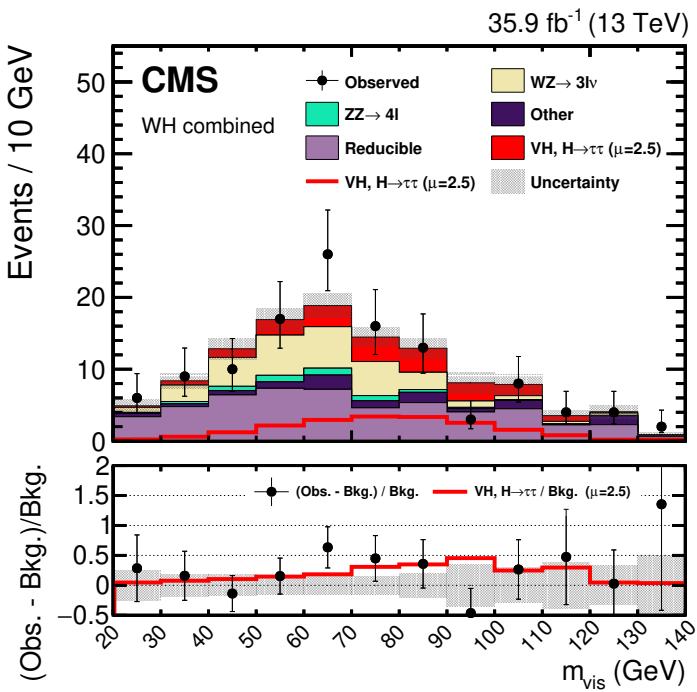
Figure 4. Post-fit visible mass distributions of the Higgs boson candidate in the four WH final states combined together. The uncertainties include both statistical and systematic components. The WH and ZH, H → ττ signal processes are summed together and shown as VH, H → ττ with a best fit $\mu = 2.5$. VH, H → ττ is shown both as a stacked filled histogram and an open overlaid histogram. The contribution from "Other" includes events from triboson, $t\bar{t}+$W/Z, $t\bar{t}$H production, and all production modes leading to H → WW and H → ZZ decays. In this distribution the WH, H → ττ process contributes 92% of the total of VH, H → ττ.

between the measured and the SM expected values for the couplings of the Higgs boson to vector bosons and to fermions, with the methods described in ref. [18]. Constraints are set with a likelihood scan that is performed for $m_H = 125$ GeV in the (κ_V,κ_f) parameter space. For this scan only, Higgs boson decays to pairs of W or Z bosons, H → WW or H → ZZ, are considered as part of the signal. All nuisance parameters are profiled for each point of the scan. As shown in figure 7, the observed likelihood contour is consistent with the SM expectations of κ_V and κ_f equal to unity providing increased confidence that the Higgs boson couples to τ leptons through a Yukawa coupling as predicted in the SM. The addition of the WH and ZH targeted final states brings roughly a 10% reduction in the maximum extent of the 68% CL for κ_V compared to the gluon fusion and vector boson fusion targeted analysis.

9 Summary

A search is presented for the standard model (SM) Higgs boson in WH and ZH associated production processes, based on data collected in proton-proton collisions by the CMS detector in 2016 at a center-of-mass energy of 13 TeV. Event categories are defined by three-lepton final states targeting WH production, and four-lepton final states targeting
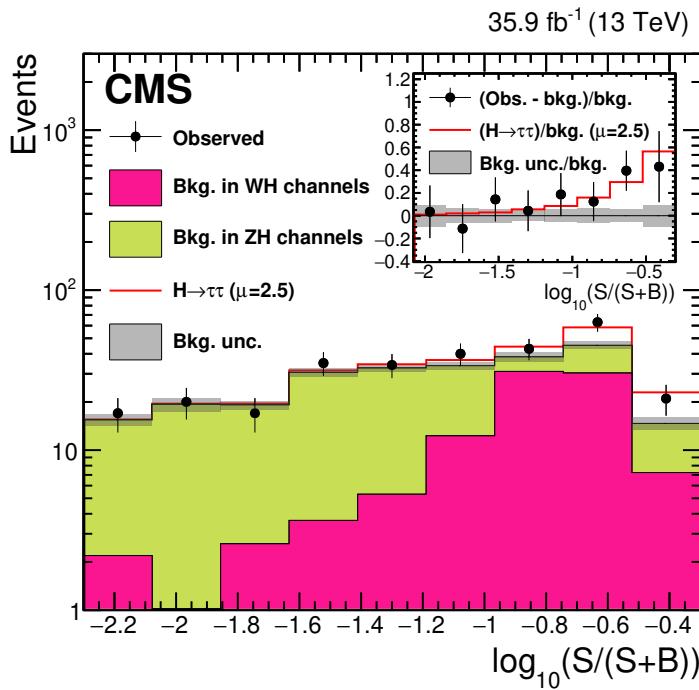
Figure 5. Distribution of the decimal logarithm of the ratio between the expected signal and the sum of the expected signal and background. The signal, corresponding to the best fit value $\mu = 2.5$, and expected background in each bin of the mass distributions used to extract the results, in all final states are combined. The background contributions are separated based on the analysis channel, WH or ZH. The inset shows the corresponding difference between the data and expected background distributions divided by the background expectation, as well as the signal expectation divided by the background expectation.

ZH production. The best fit signal strength is $\mu = 2.5^{+1.4}_{-1.3}$ ($1.0^{+1.1}_{-1.0}$ expected) for a significance of 2.3 standard deviations (1.0 expected).

The results of this analysis are combined with those of the CMS analysis targeting gluon fusion and vector boson fusion production, also performed at a center-of-mass energy of 13 TeV, and constraints on the H $\to \tau\tau$ decay rate are set. The best fit signal strength is $\mu = 1.24^{+0.29}_{-0.27}$ ($1.00^{+0.24}_{-0.23}$ expected), and the observed significance is 5.5 standard deviations (4.8 expected) for a Higgs boson mass of 125 GeV. This combination further constrains the coupling of the Higgs boson to vector bosons, resulting in measured couplings that are consistent with SM predictions within one standard deviation, providing increased confidence that the Higgs boson couples to τ leptons through a Yukawa coupling as predicted in the SM. The combination allows for extraction of the signal strengths for the four leading Higgs boson production processes using exclusively H $\to \tau\tau$ targeted final states, the results of which are largely consistent with the SM. The measurements of the Higgs boson production mechanisms using H $\to \tau\tau$ decays are the best results to date for the WH and ZH associated production mechanisms using the H $\to \tau\tau$ process.
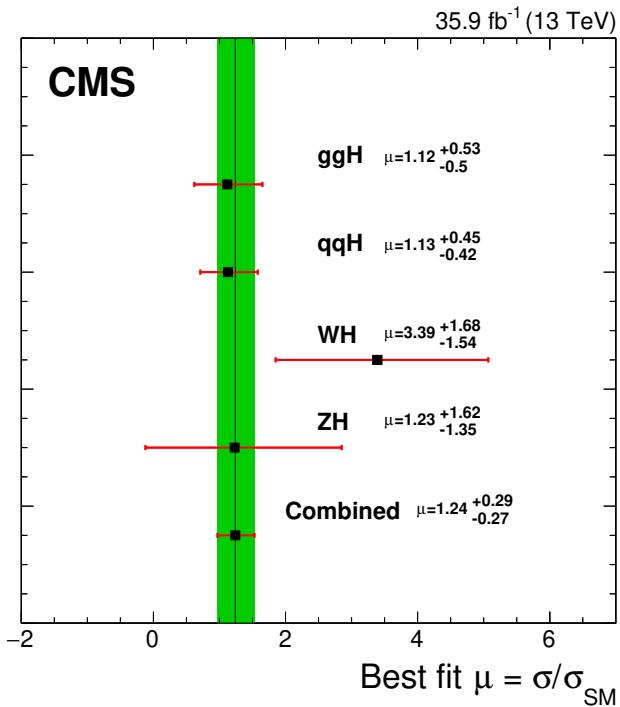
Figure 6. Best fit signal strength per Higgs boson production process, for $m_{\rm H} = 125\,\text{GeV}$, using a combination of the WH and ZH targeted analysis detailed in this paper with the CMS analysis performed in the same data set for the same decay mode but targeting the gluon fusion and vector boson fusion production mechanisms [19]. The constraints from the combined global fit are used to extract each of the individual best fit signal strengths. The combined best fit signal strength is $\mu = 1.24^{+0.29}_{-0.27}$.

Acknowledgments

Figure 7. Scans of the negative log-likelihood difference as a function of κ_V and κ_f, for $m_H = 125\,\text{GeV}$. Contours corresponding to confidence levels (CL) of 68 and 95% are shown. All nuisance parameters are profiled for each point. The scan labeled as "Combined" is a combination of the WH and ZH targeted analysis detailed in this paper with the CMS analysis performed in the same data set for the same decay mode but targeting the gluon fusion and vector boson fusion production mechanisms [19]. The results for the gluon fusion and vector boson fusion analysis are represented by the dashed lines and are labeled as "ggH + VBF". For these scans, the included $H \to WW$ and $H \to ZZ$ processes are treated as signal.

References

[1] F. Englert and R. Brout, *Broken symmetry and the mass of gauge vector mesons*, [*Phys. Rev. Lett.* **13** (1964) 321](#) [ɪɴSPIRE].

[2] P.W. Higgs, *Broken symmetries, massless particles and gauge fields*, [*Phys. Lett.* **12** (1964) 132](#) [ɪɴSPIRE].

[3] P.W. Higgs, *Broken symmetries and the masses of gauge bosons*, [*Phys. Rev. Lett.* **13** (1964) 508](#) [ɪɴSPIRE].

[4] G.S. Guralnik, C.R. Hagen and T.W.B. Kibble, *Global conservation laws and massless particles*, [*Phys. Rev. Lett.* **13** (1964) 585](#) [ɪɴSPIRE].

[5] P.W. Higgs, *Spontaneous symmetry breakdown without massless bosons*, [*Phys. Rev.* **145** (1966) 1156](#) [ɪɴSPIRE].

[6] T.W.B. Kibble, *Symmetry breaking in non-Abelian gauge theories*, [*Phys. Rev.* **155** (1967) 1554](#) [ɪɴSPIRE].

[7] ATLAS collaboration, *Observation of a new particle in the search for the Standard Model Higgs boson with the ATLAS detector at the LHC*, [*Phys. Lett.* **B 716** (2012) 1](#) [[arXiv:1207.7214](#)] [ɪɴSPIRE].

[8] CMS collaboration, *Observation of a new boson at a mass of 125 GeV with the CMS experiment at the LHC*, [*Phys. Lett.* **B 716** (2012) 30](#) [[arXiv:1207.7235](#)] [ɪɴSPIRE].

[9] CMS collaboration, *Observation of a new boson with mass near 125 GeV in pp collisions at* $\sqrt{s} = 7$ *and* $8\,TeV$, [*JHEP* **06** (2013) 081](#) [[arXiv:1303.4571](#)] [ɪɴSPIRE].

[10] ALEPH collaboration, *Observation of an excess in the search for the Standard Model Higgs boson at ALEPH*, [*Phys. Lett.* **B 495** (2000) 1](#) [[hep-ex/0011045](#)] [ɪɴSPIRE].

[11] DELPHI collaboration, *Final results from DELPHI on the searches for SM and MSSM neutral Higgs bosons*, *Eur. Phys. J.* **C 32** (2004) 145 [hep-ex/0303013] [INSPIRE].

[12] L3 collaboration, *Standard Model Higgs boson with the L3 experiment at LEP*, *Phys. Lett.* **B 517** (2001) 319 [hep-ex/0107054] [INSPIRE].

[13] OPAL collaboration, *Search for the Standard Model Higgs boson in e^+e^- collisions at $\sqrt{s} \simeq 192\,GeV$–$209\,GeV$*, *Phys. Lett.* **B 499** (2001) 38 [hep-ex/0101014] [INSPIRE].

[14] CDF collaboration, *Search for a low mass Standard Model Higgs boson in the $\tau - \tau$ decay channel in $p\bar{p}$ collisions at $\sqrt{s} = 1.96\,TeV$*, *Phys. Rev. Lett.* **108** (2012) 181804 [arXiv:1201.4880] [INSPIRE].

[15] D0 collaboration, *Search for the Standard Model Higgs boson in tau lepton pair final states*, *Phys. Lett.* **B 714** (2012) 237 [arXiv:1203.4443] [INSPIRE].

[16] ATLAS collaboration, *Evidence for the Higgs-boson Yukawa coupling to tau leptons with the ATLAS detector*, *JHEP* **04** (2015) 117 [arXiv:1501.04943] [INSPIRE].

[17] ATLAS collaboration, *Search for the Standard Model Higgs boson produced in association with a vector boson and decaying into a tau pair in pp collisions at $\sqrt{s} = 8\,TeV$ with the ATLAS detector*, *Phys. Rev.* **D 93** (2016) 092005 [arXiv:1511.08352] [INSPIRE].

[18] CMS collaboration, *Evidence for the 125 GeV Higgs boson decaying to a pair of τ leptons*, *JHEP* **05** (2014) 104 [arXiv:1401.5041] [INSPIRE].

[19] CMS collaboration, *Observation of the Higgs boson decay to a pair of τ leptons with the CMS detector*, *Phys. Lett.* **B 779** (2018) 283 [arXiv:1708.00373] [INSPIRE].

[20] CMS collaboration, *The CMS trigger system*, 2017 *JINST* **12** P01020 [arXiv:1609.02366] [INSPIRE].

[21] CMS collaboration, *The CMS experiment at the CERN LHC*, 2008 *JINST* **3** S08004 [INSPIRE].

[22] P. Nason, *A new method for combining NLO QCD with shower Monte Carlo algorithms*, *JHEP* **11** (2004) 040 [hep-ph/0409146] [INSPIRE].

[23] S. Frixione, P. Nason and C. Oleari, *Matching NLO QCD computations with parton shower simulations: the POWHEG method*, *JHEP* **11** (2007) 070 [arXiv:0709.2092] [INSPIRE].

[24] S. Alioli, P. Nason, C. Oleari and E. Re, *A general framework for implementing NLO calculations in shower Monte Carlo programs: the POWHEG BOX*, *JHEP* **06** (2010) 043 [arXiv:1002.2581] [INSPIRE].

[25] S. Alioli, K. Hamilton, P. Nason, C. Oleari and E. Re, *Jet pair production in POWHEG*, *JHEP* **04** (2011) 081 [arXiv:1012.3380] [INSPIRE].

[26] S. Alioli, P. Nason, C. Oleari and E. Re, *NLO Higgs boson production via gluon fusion matched with shower in POWHEG*, *JHEP* **04** (2009) 002 [arXiv:0812.0578] [INSPIRE].

[27] G. Luisoni, P. Nason, C. Oleari and F. Tramontano, *$HW^{\pm}/HZ + 0$ and 1 jet at NLO with the POWHEG BOX interfaced to GoSam and their merging within MiNLO*, *JHEP* **10** (2013) 083 [arXiv:1306.2542] [INSPIRE].

[28] NNPDF collaboration, *Unbiased global determination of parton distributions and their uncertainties at NNLO and at LO*, *Nucl. Phys.* **B 855** (2012) 153 [arXiv:1107.2652] [INSPIRE].

[29] D. de Florian, G. Ferrera, M. Grazzini and D. Tommasini, *Higgs boson production at the LHC: transverse momentum resummation effects in the* $H \to \gamma\gamma$, $H \to WW \to \ell\nu\ell\nu$ *and* $H \to ZZ \to 4\ell$ *decay modes*, *JHEP* **06** (2012) 132 [arXiv:1203.6321] [INSPIRE].

[30] M. Grazzini and H. Sargsyan, *Heavy-quark mass effects in Higgs boson production at the LHC*, *JHEP* **09** (2013) 129 [arXiv:1306.4581] [INSPIRE].

[31] LHC HIGGS CROSS SECTION WORKING GROUP collaboration, *Handbook of LHC Higgs cross sections: 4. Deciphering the nature of the Higgs sector*, arXiv:1610.07922 [INSPIRE].

[32] A. Denner, S. Heinemeyer, I. Puljak, D. Rebuzzi and M. Spira, *Standard Model Higgs-boson branching ratios with uncertainties*, *Eur. Phys. J.* **C 71** (2011) 1753 [arXiv:1107.5909] [INSPIRE].

[33] R.D. Ball et al., *Impact of heavy quark masses on parton distributions and LHC phenomenology*, *Nucl. Phys.* **B 849** (2011) 296 [arXiv:1101.1300] [INSPIRE].

[34] J.M. Campbell and R.K. Ellis, *MCFM for the Tevatron and the LHC*, *Nucl. Phys. Proc. Suppl.* **205-206** (2010) 10 [arXiv:1007.3492] [INSPIRE].

[35] R. Frederix and S. Frixione, *Merging meets matching in MC@NLO*, *JHEP* **12** (2012) 061 [arXiv:1209.6215] [INSPIRE].

[36] J. Alwall et al., *Comparative study of various algorithms for the merging of parton showers and matrix elements in hadronic collisions*, *Eur. Phys. J.* **C 53** (2008) 473 [arXiv:0706.2569] [INSPIRE].

[37] T. Sjöstrand et al., *An introduction to PYTHIA 8.2*, *Comput. Phys. Commun.* **191** (2015) 159 [arXiv:1410.3012] [INSPIRE].

[38] CMS collaboration, *Event generator tunes obtained from underlying event and multiparton scattering measurements*, *Eur. Phys. J.* **C 76** (2016) 155 [arXiv:1512.00815] [INSPIRE].

[39] GEANT4 collaboration, *GEANT4: a simulation toolkit*, *Nucl. Instrum. Meth.* **A 506** (2003) 250 [INSPIRE].

[40] CMS collaboration, *Particle-flow reconstruction and global event description with the CMS detector*, 2017 *JINST* **12** P10003 [arXiv:1706.04965] [INSPIRE].

[41] M. Cacciari, G.P. Salam and G. Soyez, *The anti-k_t jet clustering algorithm*, *JHEP* **04** (2008) 063 [arXiv:0802.1189] [INSPIRE].

[42] M. Cacciari, G.P. Salam and G. Soyez, *FastJet user manual*, *Eur. Phys. J.* **C 72** (2012) 1896 [arXiv:1111.6097] [INSPIRE].

[43] CMS collaboration, *Performance of electron reconstruction and selection with the CMS detector in proton-proton collisions at* $\sqrt{s} = 8\,TeV$, 2015 *JINST* **10** P06005 [arXiv:1502.02701] [INSPIRE].

[44] CMS collaboration, *Performance of the CMS muon detector and muon reconstruction with proton-proton collisions at* $\sqrt{s} = 13\,TeV$, 2018 *JINST* **13** P06015 [arXiv:1804.04528] [INSPIRE].

[45] M. Cacciari and G.P. Salam, *Dispelling the* N^3 *myth for the* k_t *jet-finder*, *Phys. Lett.* **B 641** (2006) 57 [hep-ph/0512210] [INSPIRE].

[46] CMS collaboration, *Identification of heavy-flavour jets with the CMS detector in pp collisions at* $13\,TeV$, 2018 *JINST* **13** P05011 [arXiv:1712.07158] [INSPIRE].

[47] CMS collaboration, *Reconstruction and identification of τ lepton decays to hadrons and ν_τ at CMS*, 2016 *JINST* **11** P01019 [`arXiv:1510.07488`] [INSPIRE].

[48] CMS collaboration, *Performance of reconstruction and identification of tau leptons in their decays to hadrons and tau neutrino in LHC Run-2*, CMS-PAS-TAU-16-002, CERN, Geneva, Switzerland (2016).

[49] A. Hocker et al., *TMVA — toolkit for multivariate data analysis*, in *XI Int. Workshop on Advanced Computing and Analysis Techniques in Physics Research*, CERN-OPEN-2007-007, (2007) [`physics/0703039`] [INSPIRE].

[50] CMS collaboration, *Measurement of the inclusive W and Z production cross sections in pp collisions at $\sqrt{s} = 7\,TeV$*, *JHEP* **10** (2011) 132 [`arXiv:1107.4789`] [INSPIRE].

[51] L. Bianchini, J. Conway, E.K. Friis and C. Veelken, *Reconstruction of the Higgs mass in $H \to \tau\tau$ events by dynamical likelihood techniques*, *J. Phys. Conf. Ser.* **513** (2014) 022035 [INSPIRE].

[52] CMS collaboration, *Measurements of properties of the Higgs boson decaying into the four-lepton final state in pp collisions at $\sqrt{s} = 13\,TeV$*, *JHEP* **11** (2017) 047 [`arXiv:1706.09936`] [INSPIRE].

[53] CMS collaboration, *Measurement of the cross section for top quark pair production in association with a W or Z boson in proton-proton collisions at $\sqrt{s} = 13\,TeV$*, *JHEP* **08** (2018) 011 [`arXiv:1711.02547`] [INSPIRE].

[54] CMS collaboration, *Performance of missing energy reconstruction in 13 TeV pp collision data using the CMS detector*, CMS-PAS-JME-16-004, CERN, Geneva, Switzerland (2016).

[55] CMS collaboration, *CMS luminosity measurements for the 2016 data taking period*, CMS-PAS-LUM-17-001, CERN, Geneva, Switzerland (2017).

[56] K. Hamilton, P. Nason, E. Re and G. Zanderighi, *NNLOPS simulation of Higgs boson production*, *JHEP* **10** (2013) 222 [`arXiv:1309.0017`] [INSPIRE].

The CMS collaboration

Yerevan Physics Institute, Yerevan, Armenia

A.M. Sirunyan, A. Tumasyan

Institut für Hochenergiephysik, Wien, Austria

W. Adam, F. Ambrogi, E. Asilar, T. Bergauer, J. Brandstetter, M. Dragicevic, J. Erö, A. Escalante Del Valle, M. Flechl, R. Frühwirth[1], V.M. Ghete, J. Hrubec, M. Jeitler[1], N. Krammer, I. Krätschmer, D. Liko, T. Madlener, I. Mikulec, N. Rad, H. Rohringer, J. Schieck[1], R. Schöfbeck, M. Spanring, D. Spitzbart, A. Taurok, W. Waltenberger, J. Wittmann, C.-E. Wulz[1], M. Zarucki

Institute for Nuclear Problems, Minsk, Belarus

V. Chekhovsky, V. Mossolov, J. Suarez Gonzalez

Universiteit Antwerpen, Antwerpen, Belgium

E.A. De Wolf, D. Di Croce, X. Janssen, J. Lauwers, M. Pieters, H. Van Haevermaet, P. Van Mechelen, N. Van Remortel

Vrije Universiteit Brussel, Brussel, Belgium

S. Abu Zeid, F. Blekman, J. D'Hondt, I. De Bruyn, J. De Clercq, K. Deroover, G. Flouris, D. Lontkovskyi, S. Lowette, I. Marchesini, S. Moortgat, L. Moreels, Q. Python, K. Skovpen, S. Tavernier, W. Van Doninck, P. Van Mulders, I. Van Parijs

Université Libre de Bruxelles, Bruxelles, Belgium

D. Beghin, B. Bilin, H. Brun, B. Clerbaux, G. De Lentdecker, H. Delannoy, B. Dorney, G. Fasanella, L. Favart, R. Goldouzian, A. Grebenyuk, A.K. Kalsi, T. Lenzi, J. Luetic, N. Postiau, E. Starling, L. Thomas, C. Vander Velde, P. Vanlaer, D. Vannerom, Q. Wang

Ghent University, Ghent, Belgium

T. Cornelis, D. Dobur, A. Fagot, M. Gul, I. Khvastunov[2], D. Poyraz, C. Roskas, D. Trocino, M. Tytgat, W. Verbeke, B. Vermassen, M. Vit, N. Zaganidis

Université Catholique de Louvain, Louvain-la-Neuve, Belgium

H. Bakhshiansohi, O. Bondu, S. Brochet, G. Bruno, C. Caputo, P. David, C. Delaere, M. Delcourt, A. Giammanco, G. Krintiras, V. Lemaitre, A. Magitteri, A. Mertens, M. Musich, K. Piotrzkowski, A. Saggio, M. Vidal Marono, S. Wertz, J. Zobec

Centro Brasileiro de Pesquisas Fisicas, Rio de Janeiro, Brazil

F.L. Alves, G.A. Alves, M. Correa Martins Junior, G. Correia Silva, C. Hensel, A. Moraes, M.E. Pol, P. Rebello Teles

Universidade do Estado do Rio de Janeiro, Rio de Janeiro, Brazil

E. Belchior Batista Das Chagas, W. Carvalho, J. Chinellato[3], E. Coelho, E.M. Da Costa, G.G. Da Silveira[4], D. De Jesus Damiao, C. De Oliveira Martins, S. Fonseca De Souza, H. Malbouisson, D. Matos Figueiredo, M. Melo De Almeida, C. Mora Herrera, L. Mundim, H. Nogima, W.L. Prado Da Silva, L.J. Sanchez Rosas, A. Santoro, A. Sznajder, M. Thiel, E.J. Tonelli Manganote[3], F. Torres Da Silva De Araujo, A. Vilela Pereira

Universidade Estadual Paulista [a]**, Universidade Federal do ABC** [b]**, São Paulo, Brazil**

S. Ahuja[a], C.A. Bernardes[a], L. Calligaris[a], T.R. Fernandez Perez Tomei[a], E.M. Gregores[b], P.G. Mercadante[b], S.F. Novaes[a], SandraS. Padula[a]

Institute for Nuclear Research and Nuclear Energy, Bulgarian Academy of Sciences, Sofia, Bulgaria

A. Aleksandrov, R. Hadjiiska, P. Iaydjiev, A. Marinov, M. Misheva, M. Rodozov, M. Shopova, G. Sultanov

University of Sofia, Sofia, Bulgaria

A. Dimitrov, L. Litov, B. Pavlov, P. Petkov

Beihang University, Beijing, China

W. Fang[5], X. Gao[5], L. Yuan

Institute of High Energy Physics, Beijing, China

M. Ahmad, J.G. Bian, G.M. Chen, H.S. Chen, M. Chen, Y. Chen, C.H. Jiang, D. Leggat, H. Liao, Z. Liu, F. Romeo, S.M. Shaheen[6], A. Spiezia, J. Tao, Z. Wang, E. Yazgan, H. Zhang, S. Zhang[6], J. Zhao

State Key Laboratory of Nuclear Physics and Technology, Peking University, Beijing, China

Y. Ban, G. Chen, A. Levin, J. Li, L. Li, Q. Li, Y. Mao, S.J. Qian, D. Wang, Z. Xu

Tsinghua University, Beijing, China

Y. Wang

Universidad de Los Andes, Bogota, Colombia

C. Avila, A. Cabrera, C.A. Carrillo Montoya, L.F. Chaparro Sierra, C. Florez, C.F. González Hernández, M.A. Segura Delgado

University of Split, Faculty of Electrical Engineering, Mechanical Engineering and Naval Architecture, Split, Croatia

B. Courbon, N. Godinovic, D. Lelas, I. Puljak, T. Sculac

University of Split, Faculty of Science, Split, Croatia

Z. Antunovic, M. Kovac

Institute Rudjer Boskovic, Zagreb, Croatia

V. Brigljevic, D. Ferencek, K. Kadija, B. Mesic, A. Starodumov[7], T. Susa

University of Cyprus, Nicosia, Cyprus

M.W. Ather, A. Attikis, M. Kolosova, G. Mavromanolakis, J. Mousa, C. Nicolaou, F. Ptochos, P.A. Razis, H. Rykaczewski

Charles University, Prague, Czech Republic

M. Finger[8], M. Finger Jr.[8]

Escuela Politecnica Nacional, Quito, Ecuador

E. Ayala

Universidad San Francisco de Quito, Quito, Ecuador

E. Carrera Jarrin

Academy of Scientific Research and Technology of the Arab Republic of Egypt, Egyptian Network of High Energy Physics, Cairo, Egypt

H. Abdalla[9], A.A. Abdelalim[10,11], E. Salama[12,13]

National Institute of Chemical Physics and Biophysics, Tallinn, Estonia

S. Bhowmik, A. Carvalho Antunes De Oliveira, R.K. Dewanjee, K. Ehataht, M. Kadastik, M. Raidal, C. Veelken

Department of Physics, University of Helsinki, Helsinki, Finland

P. Eerola, H. Kirschenmann, J. Pekkanen, M. Voutilainen

Helsinki Institute of Physics, Helsinki, Finland

J. Havukainen, J.K. Heikkilä, T. Järvinen, V. Karimäki, R. Kinnunen, T. Lampén, K. Lassila-Perini, S. Laurila, S. Lehti, T. Lindén, P. Luukka, T. Mäenpää, H. Siikonen, E. Tuominen, J. Tuominiemi

Lappeenranta University of Technology, Lappeenranta, Finland

T. Tuuva

IRFU, CEA, Université Paris-Saclay, Gif-sur-Yvette, France

M. Besancon, F. Couderc, M. Dejardin, D. Denegri, J.L. Faure, F. Ferri, S. Ganjour, A. Givernaud, P. Gras, G. Hamel de Monchenault, P. Jarry, C. Leloup, E. Locci, J. Malcles, G. Negro, J. Rander, A. Rosowsky, M.Ö. Sahin, M. Titov

Laboratoire Leprince-Ringuet, Ecole polytechnique, CNRS/IN2P3, Université Paris-Saclay, Palaiseau, France

A. Abdulsalam[14], C. Amendola, I. Antropov, F. Beaudette, P. Busson, C. Charlot, R. Granier de Cassagnac, I. Kucher, A. Lobanov, J. Martin Blanco, C. Martin Perez, M. Nguyen, C. Ochando, G. Ortona, P. Pigard, J. Rembser, R. Salerno, J.B. Sauvan, Y. Sirois, A.G. Stahl Leiton, A. Zabi, A. Zghiche

Université de Strasbourg, CNRS, IPHC UMR 7178, Strasbourg, France

J.-L. Agram[15], J. Andrea, D. Bloch, J.-M. Brom, E.C. Chabert, V. Cherepanov, C. Collard, E. Conte[15], J.-C. Fontaine[15], D. Gelé, U. Goerlach, M. Jansová, A.-C. Le Bihan, N. Tonon, P. Van Hove

Centre de Calcul de l'Institut National de Physique Nucleaire et de Physique des Particules, CNRS/IN2P3, Villeurbanne, France

S. Gadrat

Université de Lyon, Université Claude Bernard Lyon 1, CNRS-IN2P3, Institut de Physique Nucléaire de Lyon, Villeurbanne, France

S. Beauceron, C. Bernet, G. Boudoul, N. Chanon, R. Chierici, D. Contardo, P. Depasse, H. El Mamouni, J. Fay, L. Finco, S. Gascon, M. Gouzevitch, G. Grenier, B. Ille, F. Lagarde, I.B. Laktineh, H. Lattaud, M. Lethuillier, L. Mirabito, S. Perries, A. Popov[16], V. Sordini, G. Touquet, M. Vander Donckt, S. Viret

Georgian Technical University, Tbilisi, Georgia

T. Toriashvili[17]

Tbilisi State University, Tbilisi, Georgia

Z. Tsamalaidze[8]

RWTH Aachen University, I. Physikalisches Institut, Aachen, Germany

C. Autermann, L. Feld, M.K. Kiesel, K. Klein, M. Lipinski, M. Preuten, M.P. Rauch, C. Schomakers, J. Schulz, M. Teroerde, B. Wittmer

RWTH Aachen University, III. Physikalisches Institut A, Aachen, Germany

A. Albert, D. Duchardt, M. Erdmann, S. Erdweg, T. Esch, R. Fischer, S. Ghosh, A. Güth, T. Hebbeker, C. Heidemann, K. Hoepfner, H. Keller, L. Mastrolorenzo, M. Merschmeyer, A. Meyer, P. Millet, S. Mukherjee, T. Pook, M. Radziej, H. Reithler, M. Rieger, A. Schmidt, D. Teyssier, S. Thüer

RWTH Aachen University, III. Physikalisches Institut B, Aachen, Germany

G. Flügge, O. Hlushchenko, T. Kress, A. Künsken, T. Müller, A. Nehrkorn, A. Nowack, C. Pistone, O. Pooth, D. Roy, H. Sert, A. Stahl[18]

Deutsches Elektronen-Synchrotron, Hamburg, Germany

M. Aldaya Martin, T. Arndt, C. Asawatangtrakuldee, I. Babounikau, K. Beernaert, O. Behnke, U. Behrens, A. Bermúdez Martínez, D. Bertsche, A.A. Bin Anuar, K. Borras[19], V. Botta, A. Campbell, P. Connor, C. Contreras-Campana, V. Danilov, A. De Wit, M.M. Defranchis, C. Diez Pardos, D. Domínguez Damiani, G. Eckerlin, T. Eichhorn, A. Elwood, E. Eren, E. Gallo[20], A. Geiser, A. Grohsjean, M. Guthoff, M. Haranko, A. Harb, J. Hauk, H. Jung, M. Kasemann, J. Keaveney, C. Kleinwort, J. Knolle, D. Krücker, W. Lange, A. Lelek, T. Lenz, J. Leonard, K. Lipka, W. Lohmann[21], R. Mankel, I.-A. Melzer-Pellmann, A.B. Meyer, M. Meyer, M. Missiroli, G. Mittag, J. Mnich, V. Myronenko, S.K. Pflitsch, D. Pitzl, A. Raspereza, M. Savitskyi, P. Saxena, P. Schütze, C. Schwanenberger, R. Shevchenko, A. Singh, H. Tholen, O. Turkot, A. Vagnerini, G.P. Van Onsem, R. Walsh, Y. Wen, K. Wichmann, C. Wissing, O. Zenaiev

University of Hamburg, Hamburg, Germany

R. Aggleton, S. Bein, L. Benato, A. Benecke, V. Blobel, T. Dreyer, A. Ebrahimi, E. Garutti, D. Gonzalez, P. Gunnellini, J. Haller, A. Hinzmann, A. Karavdina, G. Kasieczka, R. Klanner, R. Kogler, N. Kovalchuk, S. Kurz, V. Kutzner, J. Lange, D. Marconi, J. Multhaup, M. Niedziela, C.E.N. Niemeyer, D. Nowatschin, A. Perieanu, A. Reimers, O. Rieger, C. Scharf, P. Schleper, S. Schumann, J. Schwandt, J. Sonneveld, H. Stadie, G. Steinbrück, F.M. Stober, M. Stöver, A. Vanhoefer, B. Vormwald, I. Zoi

Karlsruher Institut fuer Technologie, Karlsruhe, Germany

M. Akbiyik, C. Barth, M. Baselga, S. Baur, E. Butz, R. Caspart, T. Chwalek, F. Colombo, W. De Boer, A. Dierlamm, K. El Morabit, N. Faltermann, B. Freund, M. Giffels, M.A. Harrendorf, F. Hartmann[18], S.M. Heindl, U. Husemann, F. Kassel[18], I. Katkov[16], S. Kudella, S. Mitra, M.U. Mozer, Th. Müller, M. Plagge, G. Quast, K. Rabbertz, M. Schröder, I. Shvetsov, G. Sieber, H.J. Simonis, R. Ulrich, S. Wayand, M. Weber, T. Weiler, S. Williamson, C. Wöhrmann, R. Wolf

Institute of Nuclear and Particle Physics (INPP), NCSR Demokritos, Aghia Paraskevi, Greece

G. Anagnostou, G. Daskalakis, T. Geralis, A. Kyriakis, D. Loukas, G. Paspalaki, I. Topsis-Giotis

National and Kapodistrian University of Athens, Athens, Greece

B. Francois, G. Karathanasis, S. Kesisoglou, P. Kontaxakis, A. Panagiotou, I. Papavergou, N. Saoulidou, E. Tziaferi, K. Vellidis

National Technical University of Athens, Athens, Greece

K. Kousouris, I. Papakrivopoulos, G. Tsipolitis

University of Ioánnina, Ioánnina, Greece

I. Evangelou, C. Foudas, P. Gianneios, P. Katsoulis, P. Kokkas, S. Mallios, N. Manthos, I. Papadopoulos, E. Paradas, J. Strologas, F.A. Triantis, D. Tsitsonis

MTA-ELTE Lendület CMS Particle and Nuclear Physics Group, Eötvös Loránd University, Budapest, Hungary

M. Bartók[22], M. Csanad, N. Filipovic, P. Major, M.I. Nagy, G. Pasztor, O. Surányi, G.I. Veres

Wigner Research Centre for Physics, Budapest, Hungary

G. Bencze, C. Hajdu, D. Horvath[23], Á. Hunyadi, F. Sikler, T.Á. Vámi, V. Veszpremi, G. Vesztergombi[†]

Institute of Nuclear Research ATOMKI, Debrecen, Hungary

N. Beni, S. Czellar, J. Karancsi[24], A. Makovec, J. Molnar, Z. Szillasi

Institute of Physics, University of Debrecen, Debrecen, Hungary

P. Raics, Z.L. Trocsanyi, B. Ujvari

Indian Institute of Science (IISc), Bangalore, India

S. Choudhury, J.R. Komaragiri, P.C. Tiwari

National Institute of Science Education and Research, HBNI, Bhubaneswar, India

S. Bahinipati[25], C. Kar, P. Mal, K. Mandal, A. Nayak[26], D.K. Sahoo[25], S.K. Swain

Panjab University, Chandigarh, India

S. Bansal, S.B. Beri, V. Bhatnagar, S. Chauhan, R. Chawla, N. Dhingra, R. Gupta, A. Kaur, M. Kaur, S. Kaur, R. Kumar, P. Kumari, M. Lohan, A. Mehta, K. Sandeep, S. Sharma, J.B. Singh, A.K. Virdi, G. Walia

University of Delhi, Delhi, India

A. Bhardwaj, B.C. Choudhary, R.B. Garg, M. Gola, S. Keshri, Ashok Kumar, S. Malhotra, M. Naimuddin, P. Priyanka, K. Ranjan, Aashaq Shah, R. Sharma

Saha Institute of Nuclear Physics, HBNI, Kolkata, India

R. Bhardwaj[27], M. Bharti[27], R. Bhattacharya, S. Bhattacharya, U. Bhawandeep[27], D. Bhowmik, S. Dey, S. Dutt[27], S. Dutta, S. Ghosh, K. Mondal, S. Nandan, A. Purohit, P.K. Rout, A. Roy, S. Roy Chowdhury, G. Saha, S. Sarkar, M. Sharan, B. Singh[27], S. Thakur[27]

Indian Institute of Technology Madras, Madras, India

P.K. Behera

Bhabha Atomic Research Centre, Mumbai, India

R. Chudasama, D. Dutta, V. Jha, V. Kumar, P.K. Netrakanti, L.M. Pant, P. Shukla

Tata Institute of Fundamental Research-A, Mumbai, India

T. Aziz, M.A. Bhat, S. Dugad, G.B. Mohanty, N. Sur, B. Sutar, RavindraKumar Verma

Tata Institute of Fundamental Research-B, Mumbai, India

S. Banerjee, S. Bhattacharya, S. Chatterjee, P. Das, M. Guchait, Sa. Jain, S. Karmakar, S. Kumar, M. Maity[28], G. Majumder, K. Mazumdar, N. Sahoo, T. Sarkar[28]

Indian Institute of Science Education and Research (IISER), Pune, India

S. Chauhan, S. Dube, V. Hegde, A. Kapoor, K. Kothekar, S. Pandey, A. Rane, S. Sharma

Institute for Research in Fundamental Sciences (IPM), Tehran, Iran

S. Chenarani[29], E. Eskandari Tadavani, S.M. Etesami[29], M. Khakzad, M. Mohammadi Najafabadi, M. Naseri, F. Rezaei Hosseinabadi, B. Safarzadeh[30], M. Zeinali

University College Dublin, Dublin, Ireland

M. Felcini, M. Grunewald

INFN Sezione di Bari [a], **Università di Bari** [b], **Politecnico di Bari** [c], **Bari, Italy**

M. Abbrescia[a,b], C. Calabria[a,b], A. Colaleo[a], D. Creanza[a,c], L. Cristella[a,b], N. De Filippis[a,c], M. De Palma[a,b], A. Di Florio[a,b], F. Errico[a,b], L. Fiore[a], A. Gelmi[a,b], G. Iaselli[a,c], M. Ince[a,b], S. Lezki[a,b], G. Maggi[a,c], M. Maggi[a], G. Miniello[a,b], S. My[a,b], S. Nuzzo[a,b], A. Pompili[a,b], G. Pugliese[a,c], R. Radogna[a], A. Ranieri[a], G. Selvaggi[a,b], A. Sharma[a], L. Silvestris[a], R. Venditti[a], P. Verwilligen[a], G. Zito[a]

INFN Sezione di Bologna [a], **Università di Bologna** [b], **Bologna, Italy**

G. Abbiendi[a], C. Battilana[a,b], D. Bonacorsi[a,b], L. Borgonovi[a,b], S. Braibant-Giacomelli[a,b], R. Campanini[a,b], P. Capiluppi[a,b], A. Castro[a,b], F.R. Cavallo[a], S.S. Chhibra[a,b], C. Ciocca[a], G. Codispoti[a,b], M. Cuffiani[a,b], G.M. Dallavalle[a], F. Fabbri[a], A. Fanfani[a,b], E. Fontanesi,

P. Giacomelli[a], C. Grandi[a], L. Guiducci[a,b], S. Lo Meo[a], S. Marcellini[a], G. Masetti[a], A. Montanari[a], F.L. Navarria[a,b], A. Perrotta[a], F. Primavera[a,b,18], A.M. Rossi[a,b], T. Rovelli[a,b], G.P. Siroli[a,b], N. Tosi[a]

INFN Sezione di Catania [a], Università di Catania [b], Catania, Italy

S. Albergo[a,b], A. Di Mattia[a], R. Potenza[a,b], A. Tricomi[a,b], C. Tuve[a,b]

INFN Sezione di Firenze [a], Università di Firenze [b], Firenze, Italy

G. Barbagli[a], K. Chatterjee[a,b], V. Ciulli[a,b], C. Civinini[a], R. D'Alessandro[a,b], E. Focardi[a,b], G. Latino, P. Lenzi[a,b], M. Meschini[a], S. Paoletti[a], L. Russo[a,31], G. Sguazzoni[a], D. Strom[a], L. Viliani[a]

INFN Laboratori Nazionali di Frascati, Frascati, Italy

L. Benussi, S. Bianco, F. Fabbri, D. Piccolo

INFN Sezione di Genova [a], Università di Genova [b], Genova, Italy

F. Ferro[a], F. Ravera[a,b], E. Robutti[a], S. Tosi[a,b]

INFN Sezione di Milano-Bicocca [a], Università di Milano-Bicocca [b], Milano, Italy

A. Benaglia[a], A. Beschi[b], F. Brivio[a,b], V. Ciriolo[a,b,18], S. Di Guida[a,d,18], M.E. Dinardo[a,b], S. Fiorendi[a,b], S. Gennai[a], A. Ghezzi[a,b], P. Govoni[a,b], M. Malberti[a,b], S. Malvezzi[a], A. Massironi[a,b], D. Menasce[a], F. Monti, L. Moroni[a], M. Paganoni[a,b], D. Pedrini[a], S. Ragazzi[a,b], T. Tabarelli de Fatis[a,b], D. Zuolo[a,b]

INFN Sezione di Napoli [a], Università di Napoli 'Federico II' [b], Napoli, Italy, Università della Basilicata [c], Potenza, Italy, Università G. Marconi [d], Roma, Italy

S. Buontempo[a], N. Cavallo[a,c], A. De Iorio[a,b], A. Di Crescenzo[a,b], F. Fabozzi[a,c], F. Fienga[a], G. Galati[a], A.O.M. Iorio[a,b], W.A. Khan[a], L. Lista[a], S. Meola[a,d,18], P. Paolucci[a,18], C. Sciacca[a,b], E. Voevodina[a,b]

INFN Sezione di Padova [a], Università di Padova [b], Padova, Italy, Università di Trento [c], Trento, Italy

P. Azzi[a], N. Bacchetta[a], A. Boletti[a,b], A. Bragagnolo, R. Carlin[a,b], P. Checchia[a], M. Dall'Osso[a,b], P. De Castro Manzano[a], T. Dorigo[a], U. Dosselli[a], F. Gasparini[a,b], U. Gasparini[a,b], A. Gozzelino[a], S.Y. Hoh, S. Lacaprara[a], P. Lujan, M. Margoni[a,b], A.T. Meneguzzo[a,b], J. Pazzini[a,b], N. Pozzobon[a,b], P. Ronchese[a,b], R. Rossin[a,b], F. Simonetto[a,b], A. Tiko, E. Torassa[a], M. Zanetti[a,b], P. Zotto[a,b], G. Zumerle[a,b]

INFN Sezione di Pavia [a], Università di Pavia [b], Pavia, Italy

A. Braghieri[a], A. Magnani[a], P. Montagna[a,b], S.P. Ratti[a,b], V. Re[a], M. Ressegotti[a,b], C. Riccardi[a,b], P. Salvini[a], I. Vai[a,b], P. Vitulo[a,b]

INFN Sezione di Perugia [a], Università di Perugia [b], Perugia, Italy

M. Biasini[a,b], G.M. Bilei[a], C. Cecchi[a,b], D. Ciangottini[a,b], L. Fanò[a,b], P. Lariccia[a,b], R. Leonardi[a,b], E. Manoni[a], G. Mantovani[a,b], V. Mariani[a,b], M. Menichelli[a], A. Rossi[a,b], A. Santocchia[a,b], D. Spiga[a]

INFN Sezione di Pisa ^{a}, Università di Pisa ^{b}, Scuola Normale Superiore di Pisa ^{c}, Pisa, Italy

K. Androsov^a, P. Azzurri^a, G. Bagliesi^a, L. Bianchini^a, T. Boccali^a, L. Borrello, R. Castaldi^a, M.A. Ciocci^{a,b}, R. Dell'Orso^a, G. Fedi^a, F. Fiori^{a,c}, L. Giannini^{a,c}, A. Giassi^a, M.T. Grippo^a, F. Ligabue^{a,c}, E. Manca^{a,c}, G. Mandorli^{a,c}, A. Messineo^{a,b}, F. Palla^a, A. Rizzi^{a,b}, P. Spagnolo^a, R. Tenchini^a, G. Tonelli^{a,b}, A. Venturi^a, P.G. Verdini^a

INFN Sezione di Roma ^{a}, Sapienza Università di Roma ^{b}, Rome, Italy

L. Barone^{a,b}, F. Cavallari^a, M. Cipriani^{a,b}, D. Del Re^{a,b}, E. Di Marco^{a,b}, M. Diemoz^a, S. Gelli^{a,b}, E. Longo^{a,b}, B. Marzocchi^{a,b}, P. Meridiani^a, G. Organtini^{a,b}, F. Pandolfi^a, R. Paramatti^{a,b}, F. Preiato^{a,b}, S. Rahatlou^{a,b}, C. Rovelli^a, F. Santanastasio^{a,b}

INFN Sezione di Torino ^{a}, Università di Torino ^{b}, Torino, Italy, Università del Piemonte Orientale ^{c}, Novara, Italy

N. Amapane^{a,b}, R. Arcidiacono^{a,c}, S. Argiro^{a,b}, M. Arneodo^{a,c}, N. Bartosik^a, R. Bellan^{a,b}, C. Biino^a, N. Cartiglia^a, F. Cenna^{a,b}, S. Cometti^a, M. Costa^{a,b}, R. Covarelli^{a,b}, N. Demaria^a, B. Kiani^{a,b}, C. Mariotti^a, S. Maselli^a, E. Migliore^{a,b}, V. Monaco^{a,b}, E. Monteil^{a,b}, M. Monteno^a, M.M. Obertino^{a,b}, L. Pacher^{a,b}, N. Pastrone^a, M. Pelliccioni^a, G.L. Pinna Angioni^{a,b}, A. Romero^{a,b}, M. Ruspa^{a,c}, R. Sacchi^{a,b}, K. Shchelina^{a,b}, V. Sola^a, A. Solano^{a,b}, D. Soldi^{a,b}, A. Staiano^a

INFN Sezione di Trieste ^{a}, Università di Trieste ^{b}, Trieste, Italy

S. Belforte^a, V. Candelise^{a,b}, M. Casarsa^a, F. Cossutti^a, A. Da Rold^{a,b}, G. Della Ricca^{a,b}, F. Vazzoler^{a,b}, A. Zanetti^a

Kyungpook National University, Daegu, Korea

D.H. Kim, G.N. Kim, M.S. Kim, J. Lee, S. Lee, S.W. Lee, C.S. Moon, Y.D. Oh, S.I. Pak, S. Sekmen, D.C. Son, Y.C. Yang

Chonnam National University, Institute for Universe and Elementary Particles, Kwangju, Korea

H. Kim, D.H. Moon, G. Oh

Hanyang University, Seoul, Korea

J. Goh[32], T.J. Kim

Korea University, Seoul, Korea

S. Cho, S. Choi, Y. Go, D. Gyun, S. Ha, B. Hong, Y. Jo, K. Lee, K.S. Lee, S. Lee, J. Lim, S.K. Park, Y. Roh

Sejong University, Seoul, Korea

H.S. Kim

Seoul National University, Seoul, Korea

J. Almond, J. Kim, J.S. Kim, H. Lee, K. Lee, K. Nam, S.B. Oh, B.C. Radburn-Smith, S.h. Seo, U.K. Yang, H.D. Yoo, G.B. Yu

University of Seoul, Seoul, Korea

D. Jeon, H. Kim, J.H. Kim, J.S.H. Lee, I.C. Park

Sungkyunkwan University, Suwon, Korea

Y. Choi, C. Hwang, J. Lee, I. Yu

Vilnius University, Vilnius, Lithuania

V. Dudenas, A. Juodagalvis, J. Vaitkus

National Centre for Particle Physics, Universiti Malaya, Kuala Lumpur, Malaysia

I. Ahmed, Z.A. Ibrahim, M.A.B. Md Ali[33], F. Mohamad Idris[34], W.A.T. Wan Abdullah, M.N. Yusli, Z. Zolkapli

Universidad de Sonora (UNISON), Hermosillo, Mexico

J.F. Benitez, A. Castaneda Hernandez, J.A. Murillo Quijada

Centro de Investigacion y de Estudios Avanzados del IPN, Mexico City, Mexico

H. Castilla-Valdez, E. De La Cruz-Burelo, M.C. Duran-Osuna, I. Heredia-De La Cruz[35], R. Lopez-Fernandez, J. Mejia Guisao, R.I. Rabadan-Trejo, M. Ramirez-Garcia, G. Ramirez-Sanchez, R Reyes-Almanza, A. Sanchez-Hernandez

Universidad Iberoamericana, Mexico City, Mexico

S. Carrillo Moreno, C. Oropeza Barrera, F. Vazquez Valencia

Benemerita Universidad Autonoma de Puebla, Puebla, Mexico

J. Eysermans, I. Pedraza, H.A. Salazar Ibarguen, C. Uribe Estrada

Universidad Autónoma de San Luis Potosí, San Luis Potosí, Mexico

A. Morelos Pineda

University of Auckland, Auckland, New Zealand

D. Krofcheck

University of Canterbury, Christchurch, New Zealand

S. Bheesette, P.H. Butler

National Centre for Physics, Quaid-I-Azam University, Islamabad, Pakistan

A. Ahmad, M. Ahmad, M.I. Asghar, Q. Hassan, H.R. Hoorani, A. Saddique, M.A. Shah, M. Shoaib, M. Waqas

National Centre for Nuclear Research, Swierk, Poland

H. Bialkowska, M. Bluj, B. Boimska, T. Frueboes, M. Górski, M. Kazana, M. Szleper, P. Traczyk, P. Zalewski

Institute of Experimental Physics, Faculty of Physics, University of Warsaw, Warsaw, Poland

K. Bunkowski, A. Byszuk[36], K. Doroba, A. Kalinowski, M. Konecki, J. Krolikowski, M. Misiura, M. Olszewski, A. Pyskir, M. Walczak

Laboratório de Instrumentação e Física Experimental de Partículas, Lisboa, Portugal

M. Araujo, P. Bargassa, C. Beirão Da Cruz E Silva, A. Di Francesco, P. Faccioli, B. Galinhas, M. Gallinaro, J. Hollar, N. Leonardo, M.V. Nemallapudi, J. Seixas, G. Strong, O. Toldaiev, D. Vadruccio, J. Varela

Joint Institute for Nuclear Research, Dubna, Russia

S. Afanasiev, P. Bunin, M. Gavrilenko, I. Golutvin, I. Gorbunov, A. Kamenev, V. Karjavine, A. Lanev, A. Malakhov, V. Matveev[37,38], P. Moisenz, V. Palichik, V. Perelygin, S. Shmatov, S. Shulha, N. Skatchkov, V. Smirnov, N. Voytishin, A. Zarubin

Petersburg Nuclear Physics Institute, Gatchina (St. Petersburg), Russia

V. Golovtsov, Y. Ivanov, V. Kim[39], E. Kuznetsova[40], P. Levchenko, V. Murzin, V. Oreshkin, I. Smirnov, D. Sosnov, V. Sulimov, L. Uvarov, S. Vavilov, A. Vorobyev

Institute for Nuclear Research, Moscow, Russia

Yu. Andreev, A. Dermenev, S. Gninenko, N. Golubev, A. Karneyeu, M. Kirsanov, N. Krasnikov, A. Pashenkov, D. Tlisov, A. Toropin

Institute for Theoretical and Experimental Physics, Moscow, Russia

V. Epshteyn, V. Gavrilov, N. Lychkovskaya, V. Popov, I. Pozdnyakov, G. Safronov, A. Spiridonov, A. Stepennov, V. Stolin, M. Toms, E. Vlasov, A. Zhokin

Moscow Institute of Physics and Technology, Moscow, Russia

T. Aushev

National Research Nuclear University 'Moscow Engineering Physics Institute' (MEPhI), Moscow, Russia

M. Chadeeva[41], P. Parygin, D. Philippov, S. Polikarpov[41], E. Popova, V. Rusinov

P.N. Lebedev Physical Institute, Moscow, Russia

V. Andreev, M. Azarkin, I. Dremin[38], M. Kirakosyan, S.V. Rusakov, A. Terkulov

Skobeltsyn Institute of Nuclear Physics, Lomonosov Moscow State University, Moscow, Russia

A. Baskakov, A. Belyaev, E. Boos, V. Bunichev, M. Dubinin[42], L. Dudko, A. Ershov, V. Klyukhin, O. Kodolova, I. Lokhtin, I. Miagkov, S. Obraztsov, S. Petrushanko, V. Savrin, A. Snigirev

Novosibirsk State University (NSU), Novosibirsk, Russia

A. Barnyakov[43], V. Blinov[43], T. Dimova[43], L. Kardapoltsev[43], Y. Skovpen[43]

Institute for High Energy Physics of National Research Centre 'Kurchatov Institute', Protvino, Russia

I. Azhgirey, I. Bayshev, S. Bitioukov, D. Elumakhov, A. Godizov, V. Kachanov, A. Kalinin, D. Konstantinov, P. Mandrik, V. Petrov, R. Ryutin, S. Slabospitskii, A. Sobol, S. Troshin, N. Tyurin, A. Uzunian, A. Volkov

National Research Tomsk Polytechnic University, Tomsk, Russia

A. Babaev, S. Baidali, V. Okhotnikov

University of Belgrade, Faculty of Physics and Vinca Institute of Nuclear Sciences, Belgrade, Serbia

P. Adzic[44], P. Cirkovic, D. Devetak, M. Dordevic, J. Milosevic

Centro de Investigaciones Energéticas Medioambientales y Tecnológicas (CIEMAT), Madrid, Spain

J. Alcaraz Maestre, A. Álvarez Fernández, I. Bachiller, M. Barrio Luna, J.A. Brochero Cifuentes, M. Cerrada, N. Colino, B. De La Cruz, A. Delgado Peris, C. Fernandez Bedoya, J.P. Fernández Ramos, J. Flix, M.C. Fouz, O. Gonzalez Lopez, S. Goy Lopez, J.M. Hernandez, M.I. Josa, D. Moran, A. Pérez-Calero Yzquierdo, J. Puerta Pelayo, I. Redondo, L. Romero, M.S. Soares, A. Triossi

Universidad Autónoma de Madrid, Madrid, Spain

C. Albajar, J.F. de Trocóniz

Universidad de Oviedo, Oviedo, Spain

J. Cuevas, C. Erice, J. Fernandez Menendez, S. Folgueras, I. Gonzalez Caballero, J.R. González Fernández, E. Palencia Cortezon, V. Rodríguez Bouza, S. Sanchez Cruz, P. Vischia, J.M. Vizan Garcia

Instituto de Física de Cantabria (IFCA), CSIC-Universidad de Cantabria, Santander, Spain

I.J. Cabrillo, A. Calderon, B. Chazin Quero, J. Duarte Campderros, M. Fernandez, P.J. Fernández Manteca, A. García Alonso, J. Garcia-Ferrero, G. Gomez, A. Lopez Virto, J. Marco, C. Martinez Rivero, P. Martinez Ruiz del Arbol, F. Matorras, J. Piedra Gomez, C. Prieels, T. Rodrigo, A. Ruiz-Jimeno, L. Scodellaro, N. Trevisani, I. Vila, R. Vilar Cortabitarte

University of Ruhuna, Department of Physics, Matara, Sri Lanka

N. Wickramage

CERN, European Organization for Nuclear Research, Geneva, Switzerland

D. Abbaneo, B. Akgun, E. Auffray, G. Auzinger, P. Baillon, A.H. Ball, D. Barney, J. Bendavid, M. Bianco, A. Bocci, C. Botta, E. Brondolin, T. Camporesi, M. Cepeda, G. Cerminara, E. Chapon, Y. Chen, G. Cucciati, D. d'Enterria, A. Dabrowski, N. Daci, V. Daponte, A. David, A. De Roeck, N. Deelen, M. Dobson, M. Dünser, N. Dupont, A. Elliott-Peisert, P. Everaerts, F. Fallavollita[45], D. Fasanella, G. Franzoni, J. Fulcher, W. Funk, D. Gigi, A. Gilbert, K. Gill, F. Glege, M. Guilbaud, D. Gulhan, J. Hegeman, C. Heidegger, V. Innocente, A. Jafari, P. Janot, O. Karacheban[21], J. Kieseler, A. Kornmayer, M. Krammer[1], C. Lange, P. Lecoq, C. Lourenço, L. Malgeri, M. Mannelli, F. Meijers, J.A. Merlin, S. Mersi, E. Meschi, P. Milenovic[46], F. Moortgat, M. Mulders, J. Ngadiuba, S. Nourbakhsh, S. Orfanelli, L. Orsini, F. Pantaleo[18], L. Pape, E. Perez, M. Peruzzi, A. Petrilli, G. Petrucciani, A. Pfeiffer, M. Pierini, F.M. Pitters, D. Rabady, A. Racz, T. Reis, G. Rolandi[47], M. Rovere, H. Sakulin, C. Schäfer, C. Schwick, M. Seidel,

M. Selvaggi, A. Sharma, P. Silva, P. Sphicas[48], A. Stakia, J. Steggemann, M. Tosi, D. Treille, A. Tsirou, V. Veckalns[49], M. Verzetti, W.D. Zeuner

Paul Scherrer Institut, Villigen, Switzerland

L. Caminada[50], K. Deiters, W. Erdmann, R. Horisberger, Q. Ingram, H.C. Kaestli, D. Kotlinski, U. Langenegger, T. Rohe, S.A. Wiederkehr

ETH Zurich - Institute for Particle Physics and Astrophysics (IPA), Zurich, Switzerland

M. Backhaus, L. Bäni, P. Berger, N. Chernyavskaya, G. Dissertori, M. Dittmar, M. Donegà, C. Dorfer, T.A. Gómez Espinosa, C. Grab, D. Hits, T. Klijnsma, W. Lustermann, R.A. Manzoni, M. Marionneau, M.T. Meinhard, F. Micheli, P. Musella, F. Nessi-Tedaldi, J. Pata, F. Pauss, G. Perrin, L. Perrozzi, S. Pigazzini, M. Quittnat, C. Reissel, D. Ruini, D.A. Sanz Becerra, M. Schönenberger, L. Shchutska, V.R. Tavolaro, K. Theofilatos, M.L. Vesterbacka Olsson, R. Wallny, D.H. Zhu

Universität Zürich, Zurich, Switzerland

T.K. Aarrestad, C. Amsler[51], D. Brzhechko, M.F. Canelli, A. De Cosa, R. Del Burgo, S. Donato, C. Galloni, T. Hreus, B. Kilminster, S. Leontsinis, I. Neutelings, G. Rauco, P. Robmann, D. Salerno, K. Schweiger, C. Seitz, Y. Takahashi, A. Zucchetta

National Central University, Chung-Li, Taiwan

Y.H. Chang, K.y. Cheng, T.H. Doan, R. Khurana, C.M. Kuo, W. Lin, A. Pozdnyakov, S.S. Yu

National Taiwan University (NTU), Taipei, Taiwan

P. Chang, Y. Chao, K.F. Chen, P.H. Chen, W.-S. Hou, Arun Kumar, Y.F. Liu, R.-S. Lu, E. Paganis, A. Psallidas, A. Steen

Chulalongkorn University, Faculty of Science, Department of Physics, Bangkok, Thailand

B. Asavapibhop, N. Srimanobhas, N. Suwonjandee

Çukurova University, Physics Department, Science and Art Faculty, Adana, Turkey

A. Bat, F. Boran, S. Cerci[52], S. Damarseckin, Z.S. Demiroglu, F. Dolek, C. Dozen, I. Dumanoglu, S. Girgis, G. Gokbulut, Y. Guler, E. Gurpinar, I. Hos[53], C. Isik, E.E. Kangal[54], O. Kara, A. Kayis Topaksu, U. Kiminsu, M. Oglakci, G. Onengut, K. Ozdemir[55], S. Ozturk[56], B. Tali[52], U.G. Tok, H. Topakli[56], S. Turkcapar, I.S. Zorbakir, C. Zorbilmez

Middle East Technical University, Physics Department, Ankara, Turkey

B. Isildak[57], G. Karapinar[58], M. Yalvac, M. Zeyrek

Bogazici University, Istanbul, Turkey

I.O. Atakisi, E. Gülmez, M. Kaya[59], O. Kaya[60], S. Ozkorucuklu[61], S. Tekten, E.A. Yetkin[62]

Istanbul Technical University, Istanbul, Turkey

M.N. Agaras, A. Cakir, K. Cankocak, Y. Komurcu, S. Sen[63]

Institute for Scintillation Materials of National Academy of Science of Ukraine, Kharkov, Ukraine

B. Grynyov

National Scientific Center, Kharkov Institute of Physics and Technology, Kharkov, Ukraine

L. Levchuk

University of Bristol, Bristol, United Kingdom

F. Ball, L. Beck, J.J. Brooke, D. Burns, E. Clement, D. Cussans, O. Davignon, H. Flacher, J. Goldstein, G.P. Heath, H.F. Heath, L. Kreczko, D.M. Newbold[64], S. Paramesvaran, B. Penning, T. Sakuma, D. Smith, V.J. Smith, J. Taylor, A. Titterton

Rutherford Appleton Laboratory, Didcot, United Kingdom

K.W. Bell, A. Belyaev[65], C. Brew, R.M. Brown, D. Cieri, D.J.A. Cockerill, J.A. Coughlan, K. Harder, S. Harper, J. Linacre, E. Olaiya, D. Petyt, C.H. Shepherd-Themistocleous, A. Thea, I.R. Tomalin, T. Williams, W.J. Womersley

Imperial College, London, United Kingdom

R. Bainbridge, P. Bloch, J. Borg, S. Breeze, O. Buchmuller, A. Bundock, D. Colling, P. Dauncey, G. Davies, M. Della Negra, R. Di Maria, Y. Haddad, G. Hall, G. Iles, T. James, M. Komm, C. Laner, L. Lyons, A.-M. Magnan, S. Malik, A. Martelli, J. Nash[66], A. Nikitenko[7], V. Palladino, M. Pesaresi, D.M. Raymond, A. Richards, A. Rose, E. Scott, C. Seez, A. Shtipliyski, G. Singh, M. Stoye, T. Strebler, S. Summers, A. Tapper, K. Uchida, T. Virdee[18], N. Wardle, D. Winterbottom, J. Wright, S.C. Zenz

Brunel University, Uxbridge, United Kingdom

J.E. Cole, P.R. Hobson, A. Khan, P. Kyberd, C.K. Mackay, A. Morton, I.D. Reid, L. Teodorescu, S. Zahid

Baylor University, Waco, U.S.A.

K. Call, J. Dittmann, K. Hatakeyama, H. Liu, C. Madrid, B. Mcmaster, N. Pastika, C. Smith

Catholic University of America, Washington DC, U.S.A.

R. Bartek, A. Dominguez

The University of Alabama, Tuscaloosa, U.S.A.

A. Buccilli, S.I. Cooper, C. Henderson, P. Rumerio, C. West

Boston University, Boston, U.S.A.

D. Arcaro, T. Bose, D. Gastler, D. Pinna, D. Rankin, C. Richardson, J. Rohlf, L. Sulak, D. Zou

Brown University, Providence, U.S.A.

G. Benelli, X. Coubez, D. Cutts, M. Hadley, J. Hakala, U. Heintz, J.M. Hogan[67], K.H.M. Kwok, E. Laird, G. Landsberg, J. Lee, Z. Mao, M. Narain, S. Sagir[68], R. Syarif, E. Usai, D. Yu

University of California, Davis, Davis, U.S.A.

R. Band, C. Brainerd, R. Breedon, D. Burns, M. Calderon De La Barca Sanchez, M. Chertok, J. Conway, R. Conway, P.T. Cox, R. Erbacher, C. Flores, G. Funk, W. Ko, O. Kukral, R. Lander, M. Mulhearn, D. Pellett, J. Pilot, S. Shalhout, M. Shi, D. Stolp, D. Taylor, K. Tos, M. Tripathi, Z. Wang, F. Zhang

University of California, Los Angeles, U.S.A.

M. Bachtis, C. Bravo, R. Cousins, A. Dasgupta, A. Florent, J. Hauser, M. Ignatenko, N. Mccoll, S. Regnard, D. Saltzberg, C. Schnaible, V. Valuev

University of California, Riverside, Riverside, U.S.A.

E. Bouvier, K. Burt, R. Clare, J.W. Gary, S.M.A. Ghiasi Shirazi, G. Hanson, G. Karapostoli, E. Kennedy, F. Lacroix, O.R. Long, M. Olmedo Negrete, M.I. Paneva, W. Si, L. Wang, H. Wei, S. Wimpenny, B.R. Yates

University of California, San Diego, La Jolla, U.S.A.

J.G. Branson, P. Chang, S. Cittolin, M. Derdzinski, R. Gerosa, D. Gilbert, B. Hashemi, A. Holzner, D. Klein, G. Kole, V. Krutelyov, J. Letts, M. Masciovecchio, D. Olivito, S. Padhi, M. Pieri, M. Sani, V. Sharma, S. Simon, M. Tadel, A. Vartak, S. Wasserbaech[69], J. Wood, F. Würthwein, A. Yagil, G. Zevi Della Porta

University of California, Santa Barbara - Department of Physics, Santa Barbara, U.S.A.

N. Amin, R. Bhandari, J. Bradmiller-Feld, C. Campagnari, M. Citron, A. Dishaw, V. Dutta, M. Franco Sevilla, L. Gouskos, R. Heller, J. Incandela, A. Ovcharova, H. Qu, J. Richman, D. Stuart, I. Suarez, S. Wang, J. Yoo

California Institute of Technology, Pasadena, U.S.A.

D. Anderson, A. Bornheim, J.M. Lawhorn, H.B. Newman, T.Q. Nguyen, M. Spiropulu, J.R. Vlimant, R. Wilkinson, S. Xie, Z. Zhang, R.Y. Zhu

Carnegie Mellon University, Pittsburgh, U.S.A.

M.B. Andrews, T. Ferguson, T. Mudholkar, M. Paulini, M. Sun, I. Vorobiev, M. Weinberg

University of Colorado Boulder, Boulder, U.S.A.

J.P. Cumalat, W.T. Ford, F. Jensen, A. Johnson, M. Krohn, E. MacDonald, T. Mulholland, R. Patel, A. Perloff, K. Stenson, K.A. Ulmer, S.R. Wagner

Cornell University, Ithaca, U.S.A.

J. Alexander, J. Chaves, Y. Cheng, J. Chu, A. Datta, K. Mcdermott, N. Mirman, J.R. Patterson, D. Quach, A. Rinkevicius, A. Ryd, L. Skinnari, L. Soffi, S.M. Tan, Z. Tao, J. Thom, J. Tucker, P. Wittich, M. Zientek

Fermi National Accelerator Laboratory, Batavia, U.S.A.

S. Abdullin, M. Albrow, M. Alyari, G. Apollinari, A. Apresyan, A. Apyan, S. Banerjee, L.A.T. Bauerdick, A. Beretvas, J. Berryhill, P.C. Bhat, K. Burkett, J.N. Butler, A. Canepa, G.B. Cerati, H.W.K. Cheung, F. Chlebana, M. Cremonesi, J. Duarte, V.D. Elvira, J. Freeman, Z. Gecse, E. Gottschalk, L. Gray, D. Green, S. Grünendahl, O. Gutsche,

J. Hanlon, R.M. Harris, S. Hasegawa, J. Hirschauer, Z. Hu, B. Jayatilaka, S. Jindariani, M. Johnson, U. Joshi, B. Klima, M.J. Kortelainen, B. Kreis, S. Lammel, D. Lincoln, R. Lipton, M. Liu, T. Liu, J. Lykken, K. Maeshima, J.M. Marraffino, D. Mason, P. McBride, P. Merkel, S. Mrenna, S. Nahn, V. O'Dell, K. Pedro, C. Pena, O. Prokofyev, G. Rakness, L. Ristori, A. Savoy-Navarro[70], B. Schneider, E. Sexton-Kennedy, A. Soha, W.J. Spalding, L. Spiegel, S. Stoynev, J. Strait, N. Strobbe, L. Taylor, S. Tkaczyk, N.V. Tran, L. Uplegger, E.W. Vaandering, C. Vernieri, M. Verzocchi, R. Vidal, M. Wang, H.A. Weber, A. Whitbeck

University of Florida, Gainesville, U.S.A.

D. Acosta, P. Avery, P. Bortignon, D. Bourilkov, A. Brinkerhoff, L. Cadamuro, A. Carnes, M. Carver, D. Curry, R.D. Field, S.V. Gleyzer, B.M. Joshi, J. Konigsberg, A. Korytov, K.H. Lo, P. Ma, K. Matchev, H. Mei, G. Mitselmakher, D. Rosenzweig, K. Shi, D. Sperka, J. Wang, S. Wang, X. Zuo

Florida International University, Miami, U.S.A.

Y.R. Joshi, S. Linn

Florida State University, Tallahassee, U.S.A.

A. Ackert, T. Adams, A. Askew, S. Hagopian, V. Hagopian, K.F. Johnson, T. Kolberg, G. Martinez, T. Perry, H. Prosper, A. Saha, C. Schiber, R. Yohay

Florida Institute of Technology, Melbourne, U.S.A.

M.M. Baarmand, V. Bhopatkar, S. Colafranceschi, M. Hohlmann, D. Noonan, M. Rahmani, T. Roy, F. Yumiceva

University of Illinois at Chicago (UIC), Chicago, U.S.A.

M.R. Adams, L. Apanasevich, D. Berry, R.R. Betts, R. Cavanaugh, X. Chen, S. Dittmer, O. Evdokimov, C.E. Gerber, D.A. Hangal, D.J. Hofman, K. Jung, J. Kamin, C. Mills, I.D. Sandoval Gonzalez, M.B. Tonjes, H. Trauger, N. Varelas, H. Wang, X. Wang, Z. Wu, J. Zhang

The University of Iowa, Iowa City, U.S.A.

M. Alhusseini, B. Bilki[71], W. Clarida, K. Dilsiz[72], S. Durgut, R.P. Gandrajula, M. Haytmyradov, V. Khristenko, J.-P. Merlo, A. Mestvirishvili, A. Moeller, J. Nachtman, H. Ogul[73], Y. Onel, F. Ozok[74], A. Penzo, C. Snyder, E. Tiras, J. Wetzel

Johns Hopkins University, Baltimore, U.S.A.

B. Blumenfeld, A. Cocoros, N. Eminizer, D. Fehling, L. Feng, A.V. Gritsan, W.T. Hung, P. Maksimovic, J. Roskes, U. Sarica, M. Swartz, M. Xiao, C. You

The University of Kansas, Lawrence, U.S.A.

A. Al-bataineh, P. Baringer, A. Bean, S. Boren, J. Bowen, A. Bylinkin, J. Castle, S. Khalil, A. Kropivnitskaya, D. Majumder, W. Mcbrayer, M. Murray, C. Rogan, S. Sanders, E. Schmitz, J.D. Tapia Takaki, Q. Wang

Kansas State University, Manhattan, U.S.A.

S. Duric, A. Ivanov, K. Kaadze, D. Kim, Y. Maravin, D.R. Mendis, T. Mitchell, A. Modak, A. Mohammadi, L.K. Saini, N. Skhirtladze

Lawrence Livermore National Laboratory, Livermore, U.S.A.

F. Rebassoo, D. Wright

University of Maryland, College Park, U.S.A.

A. Baden, O. Baron, A. Belloni, S.C. Eno, Y. Feng, C. Ferraioli, N.J. Hadley, S. Jabeen, G.Y. Jeng, R.G. Kellogg, J. Kunkle, A.C. Mignerey, S. Nabili, F. Ricci-Tam, Y.H. Shin, A. Skuja, S.C. Tonwar, K. Wong

Massachusetts Institute of Technology, Cambridge, U.S.A.

D. Abercrombie, B. Allen, V. Azzolini, A. Baty, G. Bauer, R. Bi, S. Brandt, W. Busza, I.A. Cali, M. D'Alfonso, Z. Demiragli, G. Gomez Ceballos, M. Goncharov, P. Harris, D. Hsu, M. Hu, Y. Iiyama, G.M. Innocenti, M. Klute, D. Kovalskyi, Y.-J. Lee, P.D. Luckey, B. Maier, A.C. Marini, C. Mcginn, C. Mironov, S. Narayanan, X. Niu, C. Paus, C. Roland, G. Roland, G.S.F. Stephans, K. Sumorok, K. Tatar, D. Velicanu, J. Wang, T.W. Wang, B. Wyslouch, S. Zhaozhong

University of Minnesota, Minneapolis, U.S.A.

A.C. Benvenuti[†], R.M. Chatterjee, A. Evans, P. Hansen, J. Hiltbrand, Sh. Jain, S. Kalafut, Y. Kubota, Z. Lesko, J. Mans, N. Ruckstuhl, R. Rusack, M.A. Wadud

University of Mississippi, Oxford, U.S.A.

J.G. Acosta, S. Oliveros

University of Nebraska-Lincoln, Lincoln, U.S.A.

E. Avdeeva, K. Bloom, D.R. Claes, C. Fangmeier, F. Golf, R. Gonzalez Suarez, R. Kamalieddin, I. Kravchenko, J. Monroy, J.E. Siado, G.R. Snow, B. Stieger

State University of New York at Buffalo, Buffalo, U.S.A.

A. Godshalk, C. Harrington, I. Iashvili, A. Kharchilava, C. Mclean, D. Nguyen, A. Parker, S. Rappoccio, B. Roozbahani

Northeastern University, Boston, U.S.A.

G. Alverson, E. Barberis, C. Freer, A. Hortiangtham, D.M. Morse, T. Orimoto, R. Teixeira De Lima, T. Wamorkar, B. Wang, A. Wisecarver, D. Wood

Northwestern University, Evanston, U.S.A.

S. Bhattacharya, O. Charaf, K.A. Hahn, N. Mucia, N. Odell, M.H. Schmitt, K. Sung, M. Trovato, M. Velasco

University of Notre Dame, Notre Dame, U.S.A.

R. Bucci, N. Dev, M. Hildreth, K. Hurtado Anampa, C. Jessop, D.J. Karmgard, N. Kellams, K. Lannon, W. Li, N. Loukas, N. Marinelli, F. Meng, C. Mueller, Y. Musienko[37], M. Planer, A. Reinsvold, R. Ruchti, P. Siddireddy, G. Smith, S. Taroni, M. Wayne, A. Wightman, M. Wolf, A. Woodard

The Ohio State University, Columbus, U.S.A.

J. Alimena, L. Antonelli, B. Bylsma, L.S. Durkin, S. Flowers, B. Francis, A. Hart, C. Hill, W. Ji, T.Y. Ling, W. Luo, B.L. Winer

Princeton University, Princeton, U.S.A.

S. Cooperstein, P. Elmer, J. Hardenbrook, S. Higginbotham, A. Kalogeropoulos, D. Lange, M.T. Lucchini, J. Luo, D. Marlow, K. Mei, I. Ojalvo, J. Olsen, C. Palmer, P. Piroué, J. Salfeld-Nebgen, D. Stickland, C. Tully

University of Puerto Rico, Mayaguez, U.S.A.

S. Malik, S. Norberg

Purdue University, West Lafayette, U.S.A.

A. Barker, V.E. Barnes, S. Das, L. Gutay, M. Jones, A.W. Jung, A. Khatiwada, B. Mahakud, D.H. Miller, N. Neumeister, C.C. Peng, S. Piperov, H. Qiu, J.F. Schulte, J. Sun, F. Wang, R. Xiao, W. Xie

Purdue University Northwest, Hammond, U.S.A.

T. Cheng, J. Dolen, N. Parashar

Rice University, Houston, U.S.A.

Z. Chen, K.M. Ecklund, S. Freed, F.J.M. Geurts, M. Kilpatrick, W. Li, B.P. Padley, R. Redjimi, J. Roberts, J. Rorie, W. Shi, Z. Tu, J. Zabel, A. Zhang

University of Rochester, Rochester, U.S.A.

A. Bodek, P. de Barbaro, R. Demina, Y.t. Duh, J.L. Dulemba, C. Fallon, T. Ferbel, M. Galanti, A. Garcia-Bellido, J. Han, O. Hindrichs, A. Khukhunaishvili, P. Tan, R. Taus

Rutgers, The State University of New Jersey, Piscataway, U.S.A.

A. Agapitos, J.P. Chou, Y. Gershtein, E. Halkiadakis, M. Heindl, E. Hughes, S. Kaplan, R. Kunnawalkam Elayavalli, S. Kyriacou, A. Lath, R. Montalvo, K. Nash, M. Osherson, H. Saka, S. Salur, S. Schnetzer, D. Sheffield, S. Somalwar, R. Stone, S. Thomas, P. Thomassen, M. Walker

University of Tennessee, Knoxville, U.S.A.

A.G. Delannoy, J. Heideman, G. Riley, S. Spanier

Texas A&M University, College Station, U.S.A.

O. Bouhali[75], A. Celik, M. Dalchenko, M. De Mattia, A. Delgado, S. Dildick, R. Eusebi, J. Gilmore, T. Huang, T. Kamon[76], S. Luo, R. Mueller, D. Overton, L. Perniè, D. Rathjens, A. Safonov

Texas Tech University, Lubbock, U.S.A.

N. Akchurin, J. Damgov, F. De Guio, P.R. Dudero, S. Kunori, K. Lamichhane, S.W. Lee, T. Mengke, S. Muthumuni, T. Peltola, S. Undleeb, I. Volobouev, Z. Wang

Vanderbilt University, Nashville, U.S.A.

S. Greene, A. Gurrola, R. Janjam, W. Johns, C. Maguire, A. Melo, H. Ni, K. Padeken, J.D. Ruiz Alvarez, P. Sheldon, S. Tuo, J. Velkovska, M. Verweij, Q. Xu

University of Virginia, Charlottesville, U.S.A.

M.W. Arenton, P. Barria, B. Cox, R. Hirosky, M. Joyce, A. Ledovskoy, H. Li, C. Neu, T. Sinthuprasith, Y. Wang, E. Wolfe, F. Xia

Wayne State University, Detroit, U.S.A.

R. Harr, P.E. Karchin, N. Poudyal, J. Sturdy, P. Thapa, S. Zaleski

University of Wisconsin - Madison, Madison, WI, U.S.A.

M. Brodski, J. Buchanan, C. Caillol, D. Carlsmith, S. Dasu, L. Dodd, B. Gomber, M. Grothe, M. Herndon, A. Hervé, U. Hussain, P. Klabbers, A. Lanaro, K. Long, R. Loveless, T. Ruggles, A. Savin, V. Sharma, N. Smith, W.H. Smith, N. Woods

†: Deceased
1: Also at Vienna University of Technology, Vienna, Austria
2: Also at IRFU, CEA, Université Paris-Saclay, Gif-sur-Yvette, France
3: Also at Universidade Estadual de Campinas, Campinas, Brazil
4: Also at Federal University of Rio Grande do Sul, Porto Alegre, Brazil
5: Also at Université Libre de Bruxelles, Bruxelles, Belgium
6: Also at University of Chinese Academy of Sciences, Beijing, China
7: Also at Institute for Theoretical and Experimental Physics, Moscow, Russia
8: Also at Joint Institute for Nuclear Research, Dubna, Russia
9: Also at Cairo University, Cairo, Egypt
10: Also at Helwan University, Cairo, Egypt
11: Now at Zewail City of Science and Technology, Zewail, Egypt
12: Also at British University in Egypt, Cairo, Egypt
13: Now at Ain Shams University, Cairo, Egypt
14: Also at Department of Physics, King Abdulaziz University, Jeddah, Saudi Arabia
15: Also at Université de Haute Alsace, Mulhouse, France
16: Also at Skobeltsyn Institute of Nuclear Physics, Lomonosov Moscow State University, Moscow, Russia
17: Also at Tbilisi State University, Tbilisi, Georgia
18: Also at CERN, European Organization for Nuclear Research, Geneva, Switzerland
19: Also at RWTH Aachen University, III. Physikalisches Institut A, Aachen, Germany
20: Also at University of Hamburg, Hamburg, Germany
21: Also at Brandenburg University of Technology, Cottbus, Germany
22: Also at MTA-ELTE Lendület CMS Particle and Nuclear Physics Group, Eötvös Loránd University, Budapest, Hungary
23: Also at Institute of Nuclear Research ATOMKI, Debrecen, Hungary
24: Also at Institute of Physics, University of Debrecen, Debrecen, Hungary
25: Also at Indian Institute of Technology Bhubaneswar, Bhubaneswar, India
26: Also at Institute of Physics, Bhubaneswar, India
27: Also at Shoolini University, Solan, India
28: Also at University of Visva-Bharati, Santiniketan, India
29: Also at Isfahan University of Technology, Isfahan, Iran
30: Also at Plasma Physics Research Center, Science and Research Branch, Islamic Azad University, Tehran, Iran
31: Also at Università degli Studi di Siena, Siena, Italy
32: Also at Kyunghee University, Seoul, Korea
33: Also at International Islamic University of Malaysia, Kuala Lumpur, Malaysia
34: Also at Malaysian Nuclear Agency, MOSTI, Kajang, Malaysia
35: Also at Consejo Nacional de Ciencia y Tecnología, Mexico city, Mexico
36: Also at Warsaw University of Technology, Institute of Electronic Systems, Warsaw, Poland